PAPER

Interface behaviour of the slow diffusion equation with strong absorption: Intermediate-asymptotic properties

John R. King[1], Giles W. Richardson[2] and Jamie M. Foster[3]

[1]School of Mathematical Sciences, University of Nottingham, Nottingham, UK, [2]School of Mathematical Sciences, University of Southampton, Southampton, UK and [3]School of Mathematics and Physics, University of Portsmouth, Portsmouth, UK
Corresponding author: Jamie M. Foster; Email: jamie.michael.foster@gmail.com

Abstract
The dynamics of interfaces in slow diffusion equations with strong absorption are studied. Asymptotic methods are used to give descriptions of the behaviour local to a comprehensive range of possible singular events that can occur in any evolution. These events are: when an interface changes its direction of propagation (reversing and anti-reversing), when an interface detaches from an absorbing obstacle (detaching), when two interfaces are formed by film rupture (touchdown) and when the solution undergoes extinction. Our account of extinction and self-similar reversing and anti-reversing is built upon previous work; results on non-self-similar reversing and anti-reversing and on the various types of detachment and touchdown are developed from scratch. In all cases, verification of the asymptotic results against numerical solutions to the full PDE is provided. Self-similar solutions, both of the full equation and of its asymptotic limits, play a central role in the analysis.

1. Introduction

We shall be interested in the asymptotics of slow diffusion equations with strong absorption, that is, of PDEs of the slow diffusion (i.e. $m > 0$) form

$$\frac{\partial h}{\partial t} = \frac{\partial}{\partial x}\left(h^m \frac{\partial h}{\partial x}\right) - h^n, \tag{1.1}$$

where $h(x, t)$ is a compactly supported non-negative function, for example, the concentration of some species, with the following range of exponents

$$m + n > 1, \quad n < 1. \tag{1.2}$$

While $m + n > -1$ is sufficient for a solution to have compact support (see [4] for the special case $m = n = 0$), we shall only consider $m + n > 1$ for reasons that will become apparent; the additional condition $m + 3n + 1 > 0$ will also be imposed – again, see below. A key feature of the exponent range given in (1.2) is that both advancing and receding interfaces can occur, as can touchdown.

We shall supplement (1.1) with two different types of boundary condition. The first describes a mass-conserving free boundary located at $x = s(t)$ on the left-hand end of a one-dimensional region $x > s(t)$ in which $h > 0$. On such a boundary, we require both h and the flux to be zero, so that

$$h|_{x=s(t)} = 0, \quad h^m \frac{\partial h}{\partial x}\bigg|_{x=s(t)} = 0. \tag{1.3}$$
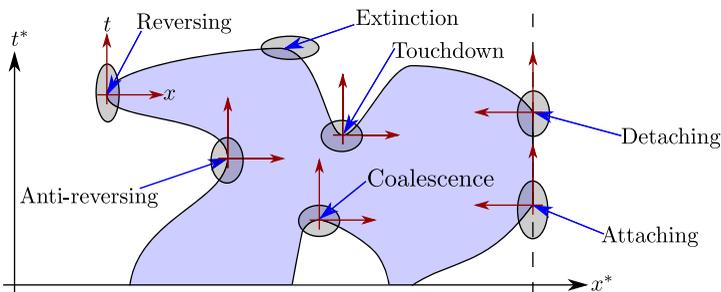
Figure 1. *A schematic of the region of support (shaded blue) for a solution for each of the behaviours (i)–(vii). The maroon axes indicate the relevant local behaviours.*

As has been shown in [9], the second of these is equivalent to imposing

$$\dot{s} = \lim_{x \searrow s(t)} \begin{cases} -h^{m-1} \dfrac{\partial h}{\partial x} & \text{if } \dot{s}(t) \le 0, \\[2ex] h^{n} \left(\dfrac{\partial h}{\partial x} \right)^{-1} & \text{if } \dot{s}(t) \ge 0. \end{cases} \tag{1.4}$$

The second type of boundary condition considered here describes scenarios in which an absorbing boundary is at a fixed location, $x = 0$ say, and takes the form

$$h|_{x=0} = 0. \tag{1.5}$$

We emphasise that, in contrast to the mass-preserving conditions (1.3), or equivalently (1.4), the absorbing boundary condition implies a non-zero flux.

Solutions local to the boundaries can exhibit a range of different behaviours depending on the exponents m and n, as well as on the initial data and boundary conditions. We shall be concerned here with various types of intermediate-asymptotic behaviour. Local to a mass-conserving interface, it is possible to observe the following: (i) what we term 'reversing' behaviour, whereby an advancing interface instantaneously pauses and then recedes [5–8];[1] (ii) the converse 'anti-reversing' behaviour, whereby a receding interface stops and then advances. Local to an absorbing boundary, governed by (1.5), we may observe (iii) 'attachment' behaviour where a mass-preserving, advancing interface arrives at an absorbing boundary, where it becomes static, with mass lost through the boundary – this case requires no detailed analysis since the solution has no knowledge of the presence of the fixed boundary prior to attachment; (iv) the converse, 'detaching' behaviour in which the interface recedes away from the absorbing boundary while obeying (1.3). Away from an interface or fixed boundary, it is possible to observe (v) 'touchdown' behaviour (often termed 'rupture' in the fluid-dynamics community) where, at an internal point, h becomes zero and two new interfaces are formed (see [15] for such behaviour in a different context). These may then recede away from one another, each governed by their own mass-conserving boundary conditions. Conversely, (vi) 'coalescence' arises when two interfaces meet one another and two disconnected regions of support merge – this also requires no detailed analysis, for a similar reason to that in (iii). Finally, (vii) 'extinction' is associated with absorption consuming all the available mass, so a region of $h > 0$ vanishes [16, 17, 22]. The local description of extinction has already been given for $m + n \ge 1$, $0 < n < 1$ in [13], as well as for $n = 1 - m$ and $0 < m < 1$ in [11, 12]. We shall briefly revisit this phenomena. A sketch of a possible evolution of the compact support in which each of

---

[1]These prior references address only the role of similarity solutions of form (1.7) below. We shall see that non-self-similar behaviour also plays a prominent role: such behaviour comprises multiple distinct components (in the sense of matched-asymptotic expansions), with similarity reductions of limit cases of the original PDE (and therefore not of the form (1.7), as set out in Section 4) playing a key role.
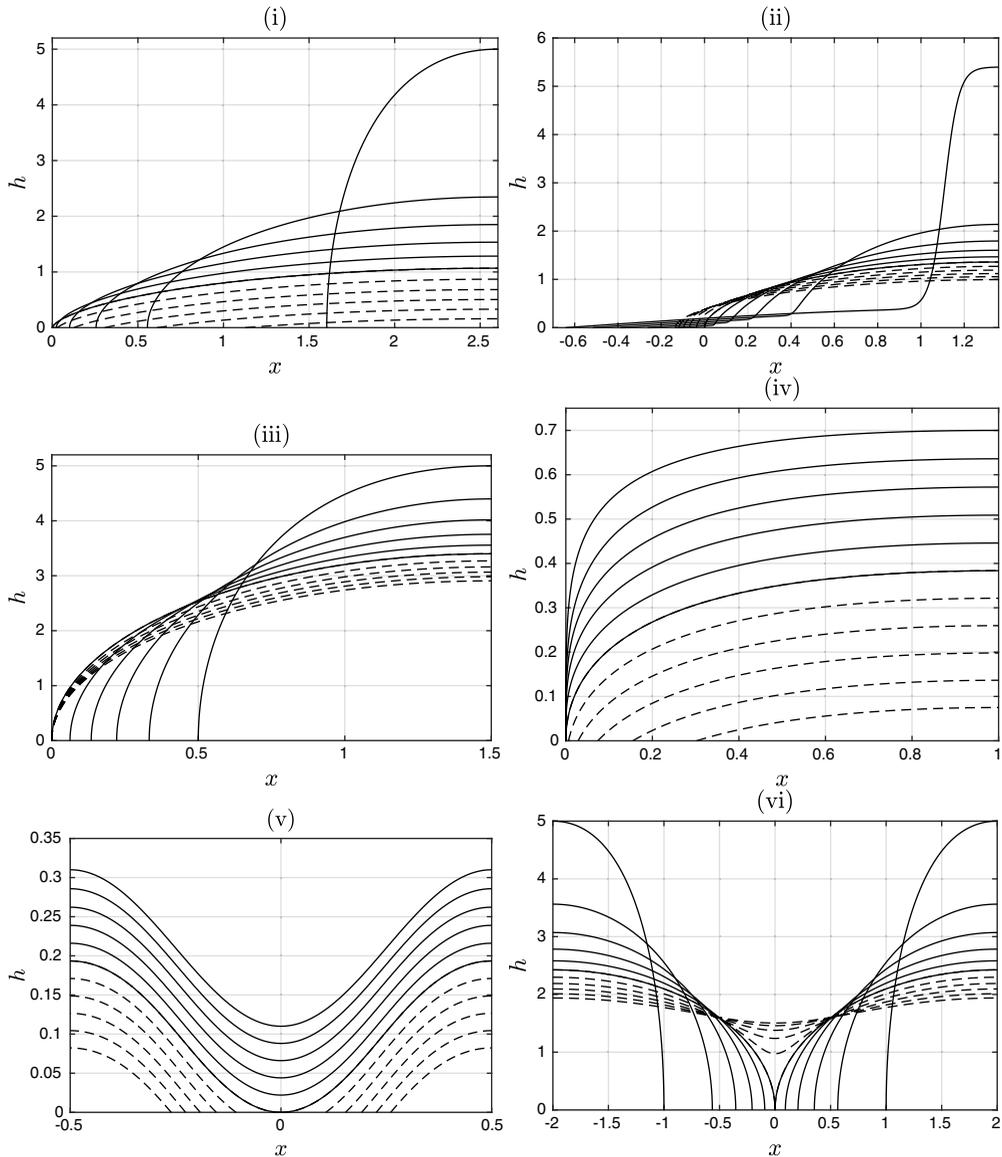
Figure 2. *Panels (i)–(vi) show numerical solutions to (1.1) exhibiting reversing, anti-reversing, attaching, detaching, touchdown and coalescence behaviour, respectively. The solid curves indicate snapshots of the solution prior to the event and the dashed curves after the event. A description of the numerical methods used to furnish these solutions is given in Section 8.*

these phenomena is shown schematically in Figure 1, and illustrative numerical solutions local to each of (i)–(vi) are shown in Figure 2.

Symmetry arguments will play a central role in what follows; see [3], for example, for relevant background. For almost all m and n (including all those in the range of interest here), the only continuous symmetries of equation (1.1) are those that are obvious by inspection, namely translations of x and of t and the scaling invariant

$$h \to \alpha h, \quad t \to \alpha^{1-n}t, \quad x \to \alpha^{(m+1-n)/2}x, \tag{1.6}$$

for arbitrary constant α. The associated similarity reductions, that is, steady states, spatially uniform solutions, travelling waves and the backward

$$h = (-t)^{\frac{1}{1-n}} f\left(x(-t)^{-\frac{m+1-n}{2(1-n)}}\right), \tag{1.7}$$

and forward

$$h = t^{\frac{1}{1-n}} f\left(xt^{-\frac{m+1-n}{2(1-n)}}\right), \tag{1.8}$$

scaling reductions associated with (1.6), will each play significant roles. The two double reductions

$$h = A_* x^{\frac{2}{m+1-n}}, \quad A_* \equiv \left(\frac{(m+1-n)^2}{2(m+1+n)}\right)^{\frac{1}{m+1-n}}, \tag{1.9}$$

(both a steady state and a scaling reduction, through (1.7) or (1.8)) and

$$h = ((1-n)(-t))^{\frac{1}{1-n}} \tag{1.10}$$

(both a spatially uniform solution and a scaling reduction, through (1.7)) play particularly prominent roles.

Other aspects related to symmetry arguments of interest in their own right but of limited relevance to the remainder of the paper are recorded in the Appendix.

Motivation and outline

A specific motivation for the current detailed study is that equation (1.1) is perhaps the simplest PDE to manifest each of the seven classes of singular behaviour noted above. Moreover, Figure 1 is evidently not specific to a particular PDE and the classification is relevant to much more general classes of moving-boundary problem; similarly, the formal-asymptotic methodologies adopted below and their consequences (notably with regard to non-generic, as well as generic, types of singular behaviour) should be of broader applicability, a point that has been recognised in other contexts, notably with regard to blow up.

The aim of the reminder of this paper is to describe the structure of solutions to (1.1) local to an event where an interface (i) reverses, (ii) anti-reverses, (iii) attaches, (iv) detaches, (v) touches down, (vi) coalesces or (vii) goes extinct. Henceforth, we shall assume that the origins of the temporal and spatial coordinates have been defined in such a way that the event of interest occurs at $t = 0$, $x = 0$. In Section 2, we discuss the different possible asymptotic behaviours local to both mass-preserving interfaces, satisfying (1.3), and absorbing boundaries, satisfying (1.5). In the subsequent section, Section 3, we examine three scenarios in which (1.1) can be reduced to an ODE namely, (a) when the solution is (quasi-)steady, (b) when the solution takes the form of a travelling wave and (c) when the solution is self-similar. Next, in Section 4, we examine the limiting behaviours in which one of the three terms in (1.1) is negligible. In Section 5, we linearise about (1.9) and (1.10) in order to establish the results needed to characterise the singular behaviours that are not of a 'pure' self-similar form. In Section 6, we revisit the self-similar solutions and carry out a detailed analysis of the phase space of the reduced ODE. In Section 7, the results of the preceding sections are leveraged in order to obtain the local behaviour of solutions immediately prior to each of the singular phenomena being investigated. In the penultimate section, Section 8, the asymptotic results are validated against direct numerical simulations of (1.1). Finally, in Section 9, we draw our conclusions.

As noted above, coalescence and attachment need no further consideration (given that we limit ourselves to the one-dimensional case), and the cases of extinction, reversing and anti-reversing have been the subject of previous analyses. Our specific goals here are to give a comprehensive and, so far as is possible, a unified description of the range of intermediate-asymptotic behaviours shown schematically in Figure 2. In so doing, we address (for the first time) touchdown and detachment, as well as describing novel non-self-similar behaviour of reversing and anti-reversing interfaces. More generally, we seek to

illustrate how a combination of self-similar and non-self-similar asymptotic structures provides a framework to analyse broad classes of moving-boundary problems – as already noted, the phenomena shown in Figure 2 are not specific to the PDE in question. That both self-similar and non-self-similar solutions arise in what follows for each scenario in question is also of more general relevance (a point to which we return in Section 9) and requires an analysis of which of the available candidates are generic (i.e. stable) – we undertake such an analysis of (1.1) for the first time.

2. Local behaviour

We now characterise the possible behaviours of (1.1) local to interfaces on which either (1.3) or (1.5) is satisfied, noting that these prove useful in what follows.

Mass-preserving interfaces.   Introducing the local variable χ about the interface

$$\chi = x - s(t), \tag{2.1}$$

with, locally, $h > 0$ in $\chi > 0$ and $h \equiv 0$ in $\chi < 0$ and applying the interface conditions (1.3) the following hold

$$h^{1-n} \sim \frac{(1-n)}{\dot{s}}\chi \quad \text{as} \quad \chi \to 0^+ \quad \text{provided} \quad \dot{s} > 0 \quad \text{(receding interface)}, \tag{2.2}$$

$$h^m \sim m(-\dot{s})\chi \quad \text{as} \quad \chi \to 0^+ \quad \text{provided} \quad \dot{s} < 0 \quad \text{(advancing interface)}. \tag{2.3}$$

The former requires that the second term in (1.1) be negligible in the limit, which, in turn, implies

$$n < 1, \quad m + n > 1. \tag{2.4}$$

The latter, (2.3), requires that the third term in (1.1) be negligible in the limit, implying that

$$m > 0, \quad m + n > 1. \tag{2.5}$$

Absorbing boundaries.   On imposing (1.5), $h|_{x=0} = 0$, the apparent sole candidate for the local behaviour neglects both the first and the third term in (1.1), and is

$$h^{m+1} \sim (m+1)Jx \quad \text{as} \quad x \searrow 0, \tag{2.6}$$

where $J(t) > 0$ is the flux through the boundary at $x = 0$. Here self-consistency requires $m > -1$ and $m + n > -1$, a condition that is automatically satisfied by our prior imposition of (1.2).

   Each of the expressions (2.2), (2.3) and (2.6) contains a single degree of freedom (s or J), as required for a second-order PDE; this conclusion is near-immediate for (2.3) and (2.6), while for (2.2) it requires an application of the Liouville-Green (JWKB) method.

3. Exact reductions to the PDE

Standard symmetry methods imply that there are three scenarios in which the PDE (1.1) can be reduced to an ODE, namely steady states, travelling waves and scaling self-similarity.

3.1. Steady states

The steady-state solutions to (1.1) satisfy

$$\frac{d}{dx}\left(h^m \frac{dh}{dx}\right) = h^n, \tag{3.1}$$
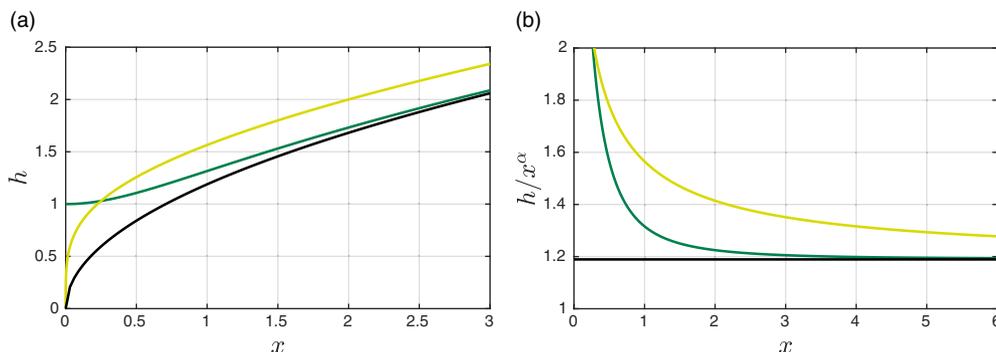
Figure 3. *Solutions to (3.1) for $m = 3$ and $n = 0$. The black curve corresponds to the exceptional solution (1.9); the yellow curve (the leaking solution) satisfies (3.6) while the green curve (the pre-touchdown) satisfies (3.8).*

an ODE that will subsequently arise as a quasi-steady balance in (1.1) for circumstances in which the time derivative is non-zero but negligible. On integrating with respect to x, we have that

$$\frac{1}{2}h^{2m}\left(\frac{dh}{dx}\right)^2 = \frac{1}{m+n+1}h^{m+n+1} + C_1, \tag{3.2}$$

for arbitrary constant C_1. Given the scaling invariance of (3.1),

$$x \mapsto \phi^{m-n+1}x, \quad h \mapsto \phi^2 h, \tag{3.3}$$

where ϕ is an arbitrary constant, we may scale $|C_1|$ in (3.2) to a convenient value. In this section, we shall set $C_1 = 0$, $C_1 = 1/2$ and $C_1 = -1/(m+n+1)$ in turn. Given (3.3), these zero, positive and negative values in effect cover the full range of possibilities, the specific values being chosen for algebraic convenience in the sense of (3.7) and (3.9) below.

The exceptional solution. For $C_1 = 0$, we have the steady solution (1.9), up to translational invariance. In Sections 3.3, 5 and 6, we shall see that it is a common component of a host of relevant solutions; owing to its significance in the remainder of the analysis, we shall refer to it as the 'exceptional solution'. Linearising (3.2) about (1.9), we obtain

$$h \sim A_* x^\alpha + \nu_1 x^{\alpha-1} + \nu_2 x^{-(m+n)\alpha} \tag{3.4}$$

where

$$\alpha = \frac{2}{m+1-n}. \tag{3.5}$$

The ν_1 term in (3.4) reflects translational invariance in x and is less singular as $x \to 0$ than the ν_2 term when $m + 3n + 1 > 0$, a condition that we impose throughout.

The leaking solution. Setting $C_1 = 1/2$ in (3.2) and imposing the interface condition (1.5) gives

$$\frac{1}{2}h^{2m}\left(\frac{dh}{dx}\right)^2 = \frac{1}{m+n+1}h^{m+n+1} + \frac{1}{2}, \quad h|_{x=0} = 0. \tag{3.6}$$

A numerical solution is shown in yellow in Figure 3. This solution, which we shall refer to as the 'leaking solution', has a unit outward flux through the origin, that is, it has the property

$$h^m\frac{dh}{dx}\bigg|_{x=0} = 1, \tag{3.7}$$

and is a candidate to form part of the asymptotic description of a solution to (1.1) that is attached to an absorbing boundary. The solution to (3.6) has asymptotic behaviour given by (3.4) as $x \to +\infty$, with v_1 and v_2 depending on m and n, the v_1 term being the dominant correction term for $m + 3n + 1 > 0$. For $n = 0$, we have the explicit solution

$$\frac{1}{m+1}h^{m+1} = \frac{1}{2}x^2 + x.$$

The pre-touchdown solution.   Finally, setting $C_1 = -1/(m+n+1)$ in (3.2) and imposing a boundary condition that requires the solution to have zero gradient at the origin leads to

$$\frac{1}{2}h^{2m}\left(\frac{dh}{dx}\right)^2 = \frac{1}{m+n+1}\left(h^{m+n+1} - 1\right), \qquad \left.\frac{dh}{dx}\right|_{x=0} = 0. \tag{3.8}$$

The solution to this problem (determined numerically) is shown in green in Figure 3. We shall refer to this solution as the 'pre-touchdown solution', and it has the property

$$h|_{x=0} = 1. \tag{3.9}$$

This solution, scaled by an appropriate function of time (i.e. in quasi-steady form), will play a role in the pre-touchdown dynamics. Once again, the solution (3.8) has the far-field behaviour (3.4). In the case $n = 0$, it has explicit solution

$$\frac{1}{m+1}h^{m+1} = \frac{1}{2}x^2 + \frac{1}{m+1}.$$

Exceptionally, the far-field behaviour of (3.8) has $v_1 = 0$ in (3.4) when $n = 0$. For $n < 0$, we have $v_1 < 0$ in (3.4) while for $n > 0$ we have $v_1 > 0$; this has implications for the intermediate-asymptotic behaviour. More precisely,

$$h^{\frac{m+1-n}{2}} \sim \frac{m+1-n}{(2(m+n+1))^{1/2}}x + \frac{n}{m+n+1}B\left(\frac{1}{2}, \frac{m+3n+1}{2(m+n+1)}\right) \quad \text{as} \quad x \to +\infty, \tag{3.10}$$

where B denotes the beta function and the constraint $m + 3n + 1 > 0$ again rears its head.

3.2. Travelling-wave solutions

Here we consider travelling-wave solutions to (1.1),

$$h = h(\zeta), \qquad \zeta = x - vt, \tag{3.11}$$

where the constant $v \neq 0$ is the wave speed. Substitution of (3.11) into (1.1) yields the ODE

$$-v\frac{dh}{d\zeta} = \frac{d}{d\zeta}\left(h^m\frac{dh}{d\zeta}\right) - h^n. \tag{3.12}$$

We shall require a solution that satisfies (1.3) at $\zeta = 0$, so that

$$h|_{\zeta=0} = 0, \qquad \left.h^m\frac{\partial h}{\partial \zeta}\right|_{\zeta=0} = 0. \tag{3.13}$$

Subsequently, for solutions with a moving interface, v will be identified with $\dot{s}$, with the travelling-wave balance (3.12), again in quasi-steady form, providing the local behaviour about the interface whenever $\dot{s} \neq 0$.

Via the rescalings

$$h \to |v|^{\frac{2}{m+n-1}}h, \qquad \zeta \to |v|^{\frac{m+1-n}{m+n-1}}\zeta \tag{3.14}$$

we can without loss of generality set $v = \pm 1$ in (3.12). The phase plane for an advancing interface ($v < 0$) is plotted in Figure 4 panel (a). The initial conditions (3.13) correspond to the sole trajectory
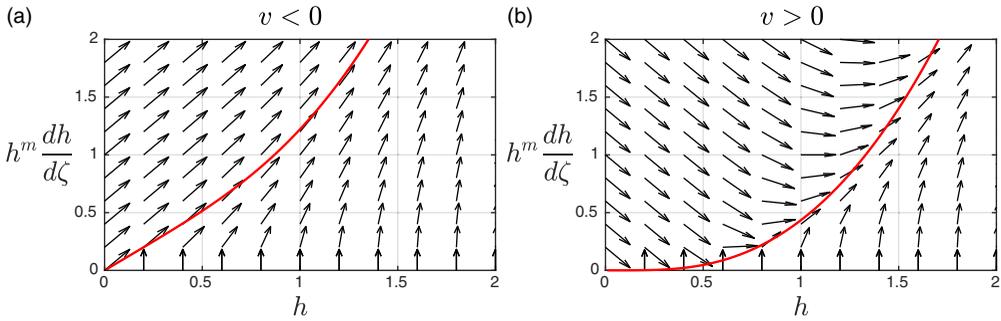
Figure 4. *Phase planes for (a) the advancing (v < 0) and (b) the receding (v > 0) travelling waves. Here m = 3 and n = 0, but qualitatively similar results apply for other exponents in the range (1.2). The red curves indicate the trajectories leaving the origin and corresponding to the solution which links the behaviours (3.15) and (3.17) in panel (a), and (3.16) and (3.17) in panel (b). Since v → −v results from ζ → −ζ in (3.12), (a) and (b) can be viewed as upper and lower quadrants of the same phase plane on also swapping the direction of the trajectories in one case. All the trajectories have the same far-field behaviour, (3.18).*

that emanates from the origin, the asymptotic behaviour of which is given in terms of the unscaled variables by

$$h \sim ((-v)m\zeta)^{1/m} \quad \text{as} \quad \zeta \to 0^+ \quad \text{with} \quad v < 0, \tag{3.15}$$

corresponding to the local behaviour (2.3). The phase plane for $v > 0$ (a receding interface) is plotted in Figure 4 panel (b). The conditions (3.13) are associated with the sole trajectory that emanates from the origin, the unscaled version of which satisfies

$$h \sim \left(\frac{(1-n)}{v} \zeta \right)^{1/(1-n)} \quad \text{as} \quad \zeta \to 0^+ \quad \text{with} \quad v > 0. \tag{3.16}$$

coinciding with (2.2).

Far-field behaviour. The phase-plane analysis demonstrates that both advancing and receding interfaces have the same far-field behaviour, with the left-hand side of (3.12) being negligible at leading order, so that

$$h \sim A_* \zeta^\alpha \quad \text{as} \quad \zeta \to +\infty. \tag{3.17}$$

We shall need a more detailed description of the behaviour; however, the relevant correction terms follow from (3.4) and from the left-hand side of (3.12) and result in the far-field behaviour

$$h \sim A_* \zeta^\alpha - vB\zeta^{\alpha-\beta} + v_1\zeta^{\alpha-1} + v_2\zeta^{-(m+n)\alpha} \quad \text{as} \quad \zeta \to +\infty, \tag{3.18}$$

where the constants β and B are given by

$$\beta = \frac{m+n-1}{m+1-n}, \quad B = \frac{(2(m+n+1))^{\frac{m-1}{m+1-n}}(m+1-n)^{\frac{3-m-n}{m+1-n}}}{(1-n)(n+m+3)}. \tag{3.19}$$

The B term is the dominant correction term in (3.18), given the condition (1.2), while v_1 and v_2 are the requisite two degrees of freedom. The phase planes confirm that the IVP (3.12)–(3.13) has a unique solution for given v, m and n; the dependencies of v_1 and v_2 upon v can be inferred from the above noted scaling property, their dependence on m and n depending on the sign of v.

In the light of these properties, and in the parameter range (1.2), the velocity of the travelling wave can thus be determined if the coefficient of the third term in far-field behaviour (3.18) is known, this being the dominant correction term in (3.18), since $\beta > 1$.

3.3. Self-similar solutions

As we shall see below, the backward self-similar reduction for (1.1),

$$h(x, t) = (-t)^{\frac{1}{1-n}} f(\xi), \quad \xi = x(-t)^{-\frac{m+1-n}{2(1-n)}} \quad \text{for} \quad t < 0, \tag{3.20}$$

coupled to the free and absorbing boundary conditions (1.3) and (1.5), provides a plausible scenario for times leading up to a singular event. As in [7], substituting (3.20) into (1.1) reveals that f satisfies the ODE

$$\frac{1}{1-n}\left(-f + \frac{m+1-n}{2} \xi \frac{df}{d\xi}\right) = \frac{d}{d\xi}\left(f^m \frac{df}{d\xi}\right) - f^n. \tag{3.21}$$

The power-law solution to (3.21) is the exceptional solution (1.9), which in similarity variables reads

$$f = A_* \xi^\alpha. \tag{3.22}$$

As a precursor to constructing solutions to (3.21) which give rise to dynamic interfaces, it is helpful to examine the possible near-field behaviours of f about the interface at $\xi = \hat{\xi}$. We find that

$$f \sim \left(\frac{m(m+1-n)\hat{\xi}}{2(1-n)}(\xi - \hat{\xi})\right)^{1/m} \quad \text{as} \quad \xi \to \hat{\xi}^+ \quad \text{for} \quad \hat{\xi} > 0, \tag{3.23}$$

$$f \sim \left(\frac{2(1-n)^2}{(m+1-n)(-\hat{\xi})}(\xi - \hat{\xi})\right)^{1/(1-n)} \quad \text{as} \quad \xi \to \hat{\xi}^+ \quad \text{for} \quad \hat{\xi} < 0 \tag{3.24}$$

are admissible. Here, $\hat{\xi} \neq 0$ is a free parameter. In the context of the original PDE, (1.1), the former behaviour corresponds to an advancing interface with $\dot{s} < 0$ (as, e.g., depicted by the solid curves in Figure 2(i), which show an advancing solution before reversing), while the latter corresponds to a receding interface with $\dot{s} > 0$. The behaviours (3.23)–(3.24) correspond to (2.2)–(2.3). In [5–7], the Liouville-Green method was used (which involves linearising about (3.23) in (3.21) and examining the self-consistent asymptotic behaviours) to demonstrate that there is only one degree of freedom in both of these behaviours, namely $\hat{\xi}$.

Even solutions satisfying

$$f \sim \hat{f} + \frac{1}{2}\hat{f}^{-m}\left(\hat{f}^n - \frac{1}{1-n}\hat{f}\right)\xi^2 \quad \text{as} \quad \xi \to 0, \tag{3.25}$$

wherein $\hat{f} > 0$ is the sole free parameter, are also of potential relevance. This behaviour clearly does not correspond to an interface of (1.1) but, in time-dependent setting, it corresponds to a point of no flux and is a candidate to describe a solution leading up to a touchdown event.

A fourth alternative is

$$f \sim K\xi^{1/(m+1)} \quad \text{as} \quad \xi \to 0^+, \tag{3.26}$$

where $K > 0$ is the sole free parameter. This leads to a static interface of (1.1) through which mass is being lost (as, e.g., depicted by the solid ones in 2(iv)). There is a final near-field behaviour of relevance, namely the exceptional solution (1.9); in view of (3.4), this contains no degrees of freedom.

The only relevant far-field behaviour for solutions to (3.21) is

$$f \sim A\xi^\alpha \quad \text{as} \quad \xi \to +\infty, \tag{3.27}$$

and it has been shown in [7] that the parameter $A > 0$ is the only degree of freedom in the large ξ behaviour. Unpicking the transformation to the self-similar variables, (3.27) corresponds to

$$h \sim Ax^\alpha \tag{3.28}$$

and is a candidate for the local behaviour as $x \to 0^+$ of the solution at $t = 0$, given that $\xi \to +\infty$ as $t \to 0^-$ at fixed x. We note that (3.27) coincides with the exceptional solution (1.9) in the case when $A = A_*$. We shall return in Section 6 to a detailed exploration of these self-similar forms.

4. Limiting cases of the PDE

Here we examine the properties (in particular, the similarity solutions) of solutions in the limiting cases in which one of the three terms in (1.1) is negligible. There are three scenarios. First, where the time derivative is negligible and the solutions are quasi-steady; the results of Section 3.1 then apply. In this section, we cover the other two cases, namely where the sink term is negligible, and where the diffusion term is negligible. Section 5 is devoted to a different class of limiting behaviour that will also prove relevant, namely linearisation about the uniform state and about the exceptional power-law solution.

4.1. Porous-medium equation balance

Neglecting the sink term in (1.1) gives the so-called porous-medium equation, *that is,*.

$$\frac{\partial h}{\partial t} \sim \frac{\partial}{\partial x}\left(h^m \frac{\partial h}{\partial x}\right) \tag{4.1}$$

the similarity solutions of which (as well as its other properties) have been very widely investigated, see, for example, [21]. We potentially need both the backward ($t < 0$) self-similar solutions

$$h \sim (-t)^\nu f_-(\eta_-), \quad \eta_- = x(-t)^{-\frac{m\nu+1}{2}} \quad \text{as} \quad t \to 0^- \quad \text{with} \quad \eta_- = O(1) \tag{4.2}$$

and the forward ($t > 0$) ones

$$h \sim t^\nu f_+(\eta_+), \quad \eta_+ = xt^{-\frac{m\nu+1}{2}} \quad \text{as} \quad t \to 0^+ \quad \text{with} \quad \eta_+ = O(1). \tag{4.3}$$

The case $\nu = 1/m$ is of most significance to us for reasons that will become clear later: in this case

$$f_-^m = m\hat{\eta}(\eta_- - \hat{\eta})_+, \qquad f_+^m = m\hat{\eta}(\eta_- + \hat{\eta})_+$$

for some constant $\hat{\eta}$; these are each both a scaling reduction and a travelling-wave solution to (4.1) and represent an exceptional connection in the phase space of f_- – see [14]. Neglect of the h^n terms as $|t| \to 0$ requires, for legitimacy, that

$$\nu < 1/(1-n), \tag{4.4}$$

which in the case $\nu = 1/m$ implies that $m + n > 1$, consistent with (1.2).

4.2. Absorption balance

The last of the three possible balances in which one of the terms in (1.1) is entirely neglected is

$$\frac{\partial h}{\partial t} \sim -h^n \tag{4.5}$$

so that

$$h^{1-n} \sim h_0^{1-n}(x) + (1-n)(-t). \tag{4.6}$$

Here, $h_0(x)$ is an arbitrary function. As we shall see, the balance (4.5) can play an asymptotic role for power law

$$h_0(x) = M|x|^{\mu/(1-n)} \tag{4.7}$$

for positive constants M and μ. In such instances, it is instructive to interpret (4.6) as backward and forward similarity reductions,

$$h = (-t)^{\frac{1}{1-n}} g_-(\omega_-), \quad \omega_- = x(-t)^{-1/\mu}, \quad g_-^{1-n} = M^{1-n}|\omega_-|^\mu + (1-n), \tag{4.8}$$

$$h = t^{\frac{1}{1-n}} g_+(\omega_+), \quad \omega_+ = xt^{-1/\mu}, \quad g_+^{1-n} = M^{1-n}|\omega_+|^\mu - (1-n), \tag{4.9}$$

from which it is clear that self-consistency as $|t| \to 0$ in the neglect of the diffusion term in (1.1) requires

$$\mu m + (\mu - 2)(1 - n) > 0. \tag{4.10}$$

5. Linearisations

In this section, we linearise about two special solutions to (1.1), namely the uniform solution (1.10) and exceptional power-law solution (1.9). The analysis of Section 7 is devoted to characterising which of the possible candidates identified in Sections 3–6 can in fact be realised in describing the various types of singular behaviour.

5.1. Linearisation about the uniform state

We linearise about the uniform state, (1.10), by setting

$$h \sim ((1 - n)(-t))^{1/(1-n)} + \mathcal{H}(x, t) \tag{5.1}$$

in (1.1) and neglect nonlinear terms in $\mathcal{H}$ to give

$$\frac{\partial \mathcal{H}}{\partial t} = ((1 - n)(-t))^{m/(1-n)} \frac{\partial^2 \mathcal{H}}{\partial x^2} - \frac{n}{(1 - n)(-t)} \mathcal{H}. \tag{5.2}$$

Defining

$$\mathcal{H} = (-t)^{\frac{n}{1-n}} \mathcal{G}(x, \tau), \quad -\tau = \frac{((1 - n)(-t))^{\frac{m+1-n}{1-n}}}{m + 1 - n} \tag{5.3}$$

transforms (5.2) to the heat equation

$$\frac{\partial \mathcal{G}}{\partial \tau} = \frac{\partial^2 \mathcal{G}}{\partial x^2}. \tag{5.4}$$

The backward self-similar solutions without exponential growth as $|x| \to +\infty$ are given by the Hermite polynomials H_k, namely

$$\mathcal{G} = C_k(-\tau)^{k/2} H_k \left(x(-\tau)^{-1/2}/2 \right) \tag{5.5}$$

where k is a non-negative integer and C_k is some constant.[2]

The following properties will be needed in due course. Firstly, (5.3)–(5.5) require, for the self-consistency of (5.1) (*i.e.* that the second term therein be negligible in comparison to the first in the limit that $t \to 0^-$), that

$$km + (k - 2)(1 - n) > 0; \tag{5.6}$$

the case $k = 0$ is therefore always excluded, unsurprisingly since it simply corresponds to a translation in t. Secondly, a standard result for H_k implies that (5.5) renders the matching condition

$$\mathcal{H}(x, t) \sim C_k(-t)^{-\frac{n}{1-n}} x^k \quad \text{as} \quad |x(-\tau)^{-1/2}| \to \infty, \tag{5.7}$$

so that

$$h^{1-n} \sim (1 - n)(-t) + (1 - n)^{\frac{1-2n}{1-n}} C_k x^k, \tag{5.8}$$

cf. (4.6), with (5.6) then corresponding to (4.10).

---

[2]We note that $f = (1 - n)^{\frac{1}{1-n}}$ is of course an exact solution to (3.21) and that the length scales associated both with (3.20) and with (5.3) and (5.5) are $x \propto (-t)^{\frac{m+1-n}{2(1-n)}}$.

5.2. Linearisation about the exceptional solution

The other linearised problem that we shall need to characterise is that about the exceptional solution, (1.9). On setting

$$h \sim A_* x^\alpha + \bar{\mathcal{H}}(x, t) \tag{5.9}$$

in (1.1), linearising in $\bar{\mathcal{H}}$ gives

$$\frac{\partial \bar{\mathcal{H}}}{\partial t} = A_*^m \frac{\partial^2}{\partial x^2} \left(x^{m\alpha} \bar{\mathcal{H}} \right) - n A_*^{-(1-n)} x^{-(1-n)\alpha} \bar{\mathcal{H}}. \tag{5.10}$$

Elucidating the behaviour of solutions to (5.10) will provide information crucial to what follows, specifically with regard to backward self-similarity. In order to analyse the linear problem (5.10), it is helpful to use the definitions of A_* and α to rewrite it in the form

$$x^{2-m\alpha} \frac{\partial \bar{\mathcal{H}}}{\partial t} = A_*^m \left(x^{2-m\alpha} \frac{\partial^2}{\partial x^2} \left(x^{m\alpha} \bar{\mathcal{H}} \right) - (\alpha(m+1) - 2)(\alpha(m+1) - 1)\bar{\mathcal{H}} \right). \tag{5.11}$$

The right-hand side of (5.11) dominates as $x \to 0$, since $2 - m\alpha > 0$ in the range of parameters that we consider, (1.2). The possible solution behaviours are thus found by neglecting the left-hand side of (5.11) and solving the resulting Euler equation in x for $\bar{\mathcal{H}}$; these are

$$\bar{\mathcal{H}} \sim \nu_1(t) x^{\alpha-1}, \qquad \bar{\mathcal{H}} \sim \nu_2(t) x^{-(m+n)\alpha}, \tag{5.12}$$

where $\nu_1(t)$ and $\nu_2(t)$ are arbitrary functions, as in (3.4). There are two distinct cases to be considered: for $m + 3n + 1 > 0$, the second of (5.12) is the more singular so it is natural to specify

$$\bar{\mathcal{H}} = o \left(x^{-(2m+1)\alpha+2} \right) \quad \text{as} \quad x \to 0^+ \quad \text{if} \quad m + 3n + 1 > 0 \tag{5.13}$$

as a boundary condition on (5.10), the local behaviour then being given by the first of (5.12), corresponding to a (small) translation of x in (5.9). By contrast, if $m + 3n + 1 < 0$ the first of (5.12) is the more singular so it is natural instead to specify

$$\bar{\mathcal{H}} = o \left(x^{\alpha-1} \right) \quad \text{as} \quad x \to 0^+ \quad \text{if} \quad m + 3n + 1 < 0. \tag{5.14}$$

As already noted, henceforth we only consider the case $m + 3n + 1 > 0$, so that (5.13) applies (though in (II) below we record an instructive result for $m + 3n + 1 < 0$); the analysis of the converse case proceeds on similar lines, but will be omitted here (in part because it appears of less physical relevance).

Two transformations, (I) and (II) below, reduce (5.10) to standard forms. In both cases, we define

$$r = x^{\frac{2-m\alpha}{2}}, \tag{5.15}$$

the definitions of G_i being guided by (5.12). We have

$$\text{(I):} \quad \bar{\mathcal{H}}(x, t) = x^{\alpha-1} G_1(r, t), \quad m + 3n + 1 > 0, \tag{5.16}$$

$$\frac{\partial G_1}{\partial t} = \frac{1}{4}(2 - m\alpha)^2 A_*^m \left(\frac{\partial^2 G_1}{\partial r^2} + \frac{N_1 - 1}{r} \frac{\partial G_1}{\partial r} \right), \quad N_1 = 2\frac{(m+2)\alpha - 1}{2 - m\alpha}. \tag{5.17}$$

$$\text{(II):} \quad \bar{\mathcal{H}}(x, t) = x^{-(m+n)\alpha} G_2(r, t), \quad m + 3n + 1 < 0, \tag{5.18}$$

$$\frac{\partial G_2}{\partial t} = \frac{1}{4}(2 - m\alpha)^2 A_*^m \left(\frac{\partial^2 G_2}{\partial r^2} + \frac{N_2 - 1}{r} \frac{\partial G_2}{\partial r} \right), \quad N_2 = 2\frac{5 - (3m+2)\alpha}{2 - m\alpha}. \tag{5.19}$$

These representations allow application of standard theory for the radially symmetric heat equation.[3] As was pursued in [5], the standard forms for the backward similarity solutions to (5.17) and (5.19) are

$$G = (-t)^M g(y), \quad y = \frac{2r}{A_*^{m/2}(2 - m\alpha)(-t)^{1/2}} \tag{5.20}$$

(where M is an arbitrary constant) and satisfy

$$z\frac{d^2 g}{dz^2} + \left(\frac{N}{2} - z\right)\frac{dg}{dz} + Mg = 0, \quad z = y^2, \tag{5.21}$$

so that the solutions having the necessary regularity as $z \to 0$ (namely g finite as $z \to 0$) and growing algebraically, rather than exponentially (of the form $\log g \sim z$ as $z \to +\infty$), as $z \to +\infty$ are given by the generalised Laguerre polynomials,

$$g \propto L_P^{(N-2)/2}(z), \tag{5.22}$$

where $P = M + (N - 2)/2$; since $(N - 2)/2$ need not be an integer, this is not the standard case, but M is required to be a positive integer, leading to g being an M-th order polynomial in z (i.e. in (5.20)–(5.21), M should be viewed as an eigenvalue, leading to the requirement that it be a non-negative integer). The first few eigenmodes (radially symmetric heat polynomials, representing a complete set of eigenmodes) are thus multiples of the following:

$$M = 0, \quad g_0 = 1, \tag{5.23}$$

$$M = 1, \quad g_1 = z - N/2, \tag{5.24}$$

$$M = 2, \quad g_2 = z^2 - (N + 2)z + N(N + 2)/4, \tag{5.25}$$

$$M = 3, \quad g_3 = z^3 - 3(N + 4)z^2/2 + 3(N + 2)(N + 4)z/4 - N(N + 2)(N + 4)/8. \tag{5.26}$$

We shall subsequently need to view the leading term in (5.9) as a similarity solution of the form (4.9), while in case (I) above (5.20) implies that $\bar{\mathcal{H}}$ is of the self-similar form

$$\bar{\mathcal{H}} = (-t)^L F(\xi), \quad \text{where} \quad L = M + \frac{1 + n - m}{2(1 - n)}, \tag{5.27}$$

so self-consistency of (5.9) requires that

$$M > \frac{m + 1 - n}{2(1 - n)}. \tag{5.28}$$

Hence, $M = 0$ and $M = 1$ are excluded (in the latter case (5.28) would require $m + n < 1$ for $n < 1$, again identifying familiar borderline cases). This is to be expected in view of the invariance of (1.1) under translations of x and t, illustrating a more general principle (we touch on some of the broader implications in Section 9). Equation (5.10) inherits t, but not x, translation invariance, and we pursue the reasoning in two stages. It follows from t translation invariance that the Mth mode is proportional to the time derivative of the $(M + 1)$th mode, so that

$$g_M \propto z\frac{dg_{M+1}}{dz} - (M + 1)g_{M+1}. \tag{5.29}$$

Hence, we have

$$\bar{\mathcal{H}}(x, t + t_0) = \sum_{k=0}^{M} a_{k,M} t_0^k \bar{\mathcal{H}}_{M-k}(x, t) \tag{5.30}$$

---

[3]Here $N_1 + N_2 = 4$, which has as a special case the well-known transformation between the spherically symmetric heat equation and that in a single Cartesian dimension (there being a nonlinear generalisation – see [18]). $N_1 > 2$ applies for $m + 3n + 1 > 0$ and $N_2 > 2$ for $m + 3n + 1 < 0$; the borderline case $m + 3n + 1 = 0$ is characterised by $N_1 = N_2 = 2$, as is to be expected.

(where $\bar{\mathcal{H}}_p$ is the solution to (5.10) associated with g_p) with

$$a_{0,M} = 1, \quad a_{k,M} = \prod_{L=0}^{k-1} \alpha_{M-L}/k!, \quad k \geq 1, \tag{5.31}$$

where

$$\bar{\mathcal{H}}_{M-1}(x,t) = \alpha_M \frac{\partial}{\partial t} \bar{\mathcal{H}}_M(x,t). \tag{5.32}$$

Writing the solution to (5.10) in the form

$$\bar{\mathcal{H}} \sim \sum_{p=0}^{\infty} K_p \bar{\mathcal{H}}_p(x,t), \tag{5.33}$$

if we now choose t_0 in (5.30) such that

$$K_1 = \sum_{M=1}^{\infty} a_{M-1,M} t_0^{M-1} \tag{5.34}$$

then the time-translated version of $\mathcal{H}$ has $K_1 = 0$. This translation will modify the value of K_0, but here x translation invariance comes into play: since $\bar{\mathcal{H}}_0 \propto dx^\alpha/dx$, translating suitably in (5.9) allows K_0 also to be set to zero.

The condition (5.28) will play a crucial role in what follows, the borderline cases

$$m = (2M - 1)(1 - n), \qquad M = 2, 3, \cdots \tag{5.35}$$

identifying the bifurcation points in Figure 7 below.

6. Self-similar bifurcation diagram

6.1. Backward self-similarity

We now analyse in detail some of the phase space of the ODE (3.21) associated with the full backward similarity reduction (1.7) of the PDE (1.1). In order to construct solutions to the ODE (3.21) that give rise to viable dynamic solutions to (1.1), it remains to determine whether it is possible to connect one of the near-field behaviours (3.23)–(3.26) with the far-field behaviour (3.27). We shall address this question by setting up an IVP (i.e. a shooting problem) from $\xi = \infty$. It was proved in Lemma 4.4 of [6] that trajectories emanating from (3.27) with $A > 0$ will, when integrated in the direction of decreasing ξ, either reach $f = 0$ or $f^m df/d\xi = 0$ at some finite ξ. In lieu of an analytical means to solve the connection problem, the result from [6] motivates its numerical study by means of a shooting scheme in which $A > 0$ is varied as the shooting parameter. Once a value for A has been adopted, the behaviour (3.27) can be used to set initial conditions to integrate (3.21) backwards in ξ, and this process can be terminated at the value $\xi = \xi_{\text{term}}$ at which $f = 0$ or $f^m df/d\xi = 0$ (whichever occurs first). Once this has been done, it is then possible to assess whether one of the behaviours (3.23)–(3.26) has been reached by reading off the values of $f|_{\xi=\xi_{\text{term}}}, f^m df/d\xi|_{\xi=\xi_{\text{term}}}$ and ξ_{term}. If the integration stopped at a point where

(a) $f|_{\xi=\xi_{\text{term}}} = 0, f^m \left.\dfrac{df}{d\xi}\right|_{\xi=\xi_{\text{term}}} = 0$ with $\xi_{\text{term}} > 0$, the behaviour (3.23) has been attained,

(b) $f|_{\xi=\xi_{\text{term}}} = 0, f^m \left.\dfrac{df}{d\xi}\right|_{\xi=\xi_{\text{term}}} = 0$ with $\xi_{\text{term}} < 0$, the behaviour (3.24) has been attained,

(c) $f|_{\xi=\xi_{\text{term}}} > 0, f^m \left.\dfrac{df}{d\xi}\right|_{\xi=\xi_{\text{term}}} = 0$ with $\xi_{\text{term}} = 0$, the behaviour (3.25) has been attained,

(d) $f|_{\xi=\xi_{\text{term}}} = 0, f^m \left.\dfrac{df}{d\xi}\right|_{\xi=\xi_{\text{term}}} > 0$ with $\xi_{\text{term}} = 0$, the behaviour (3.26) has been attained.
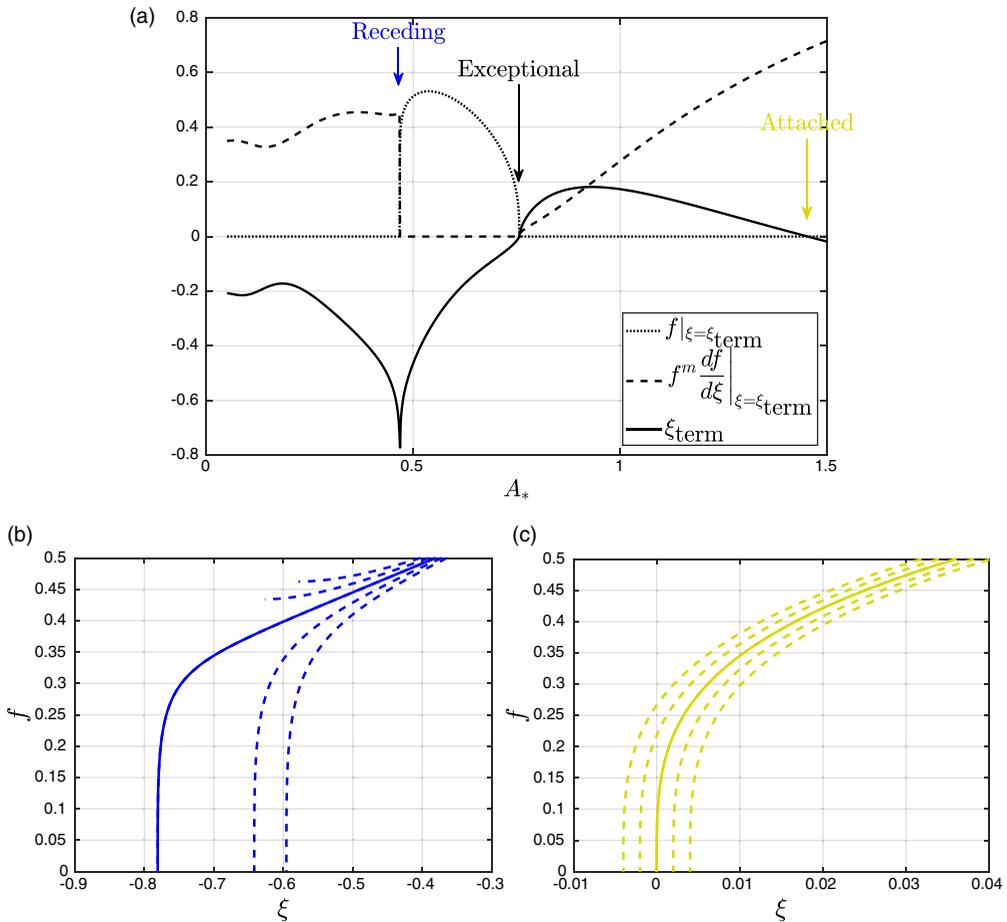
Figure 5. *Results of the shooting scheme to detect viable solutions (3.21) for $m = 2.5$ and $n = 0$. The upper panel, (a), shows the variation of f, $f^m df/d\xi$ and ξ_{term} at the termination point ($\xi = \xi_{term}$) with the shooting parameter A. Candidate receding, exceptional and attached trajectories are indicated by the blue, black and yellow arrows, respectively. The lower panels, (b) and (c), show the candidate receding and attached trajectories (solid curves), respectively, along with a few trajectories 'near' to these candidates (dashed curves) – "near" in the sense that they have values of A close to the candidates.*

The additional constraints in (a)–(d), namely a pair of boundary conditions in (a) and (b) and the requirement that ξ_{term} be zero in (c) and (d), lead to the selection of a discrete set of admissible values of A for given m and n, as exemplified in Figure 7. The results of this shooting scheme are summarised in Figures 5 and 6 for $m = 2.5$, $n = 0$ and $m = 4.5$, $n = 0$, respectively. Similar bifurcation diagrams have been presented in the authors' previous work, [5, 6], but this is the first time that solutions reaching states (c) or (d) have been found. In the former case, one viable solution with a receding interface (blue), satisfying (3.24), was identified, as well as one with an attached interface (yellow), satisfying (3.26). In the latter case, two viable solutions were found, one with the local behaviour (3.26), which is a potential profile prior to touchdown (green), and another with an advancing interface (red) and the near-field behaviour (3.23). Similar experiments were carried out for many values of $m \in (1, 8)$ while retaining $n = 0$ and the locations of the viable solutions are summarised in the top right panel of Figure 7. Further computations were carried out for other values of n, namely -1, $-1/2$ and $1/2$, and similar results were found, see the other panels in Figure 7. In summary, we observe that for a particular pair of values

(a)

(b)   (c)
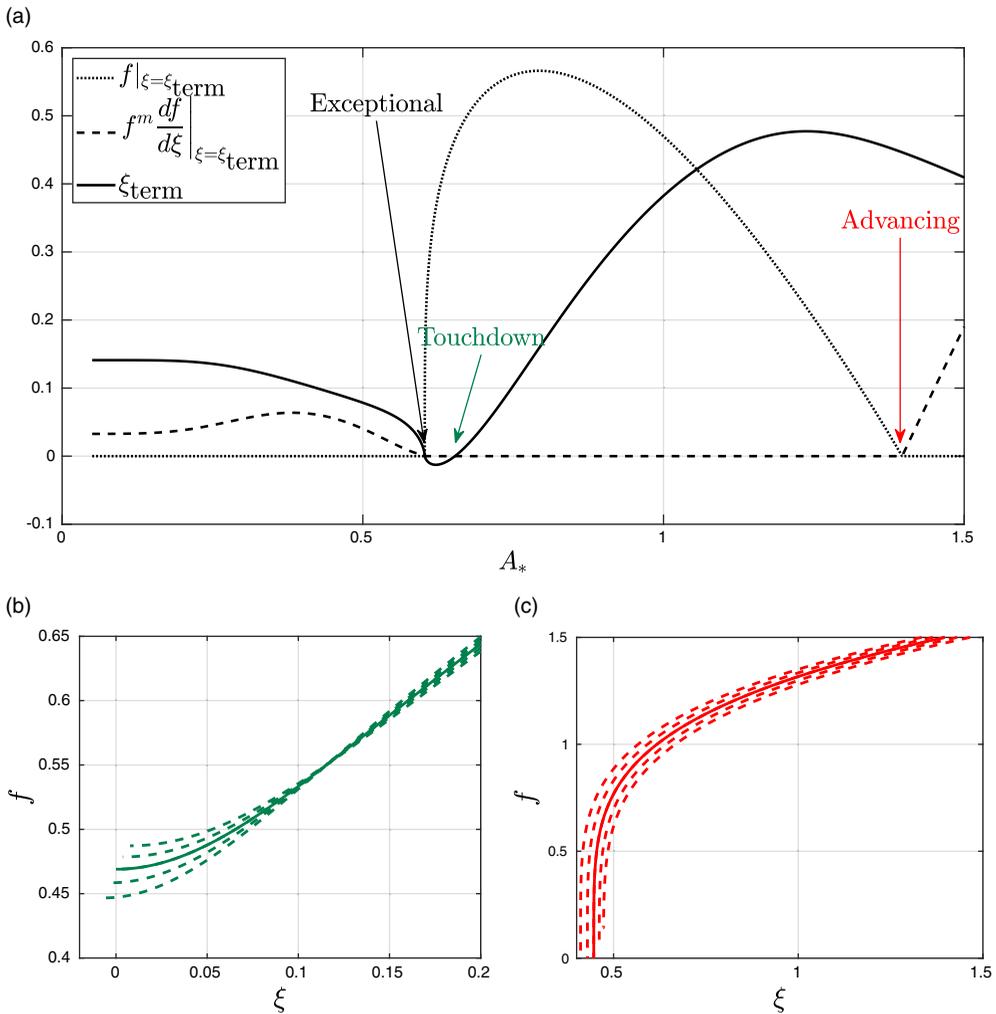
Figure 6. *Results of the shooting scheme to detect viable solutions (3.21) for $m = 4.5$ and $n = 0$. The upper panel, (a), shows the variation of f, $f^m df/d\xi$ and ξ_{term} at the termination point ($\xi = \xi_{term}$) with the shooting parameter A_*. Candidate exceptional, touchdown and advancing trajectories are indicated by the black, green and red arrows, respectively. The lower panels, (b) and (c), show the candidate touchdown and attached trajectories (solid curves), respectively, along with a few trajectories 'near' to these candidates (dashed curves).*

of m and n it is possible to find connections between the far-field behaviour (3.27) and the near-field behaviours (3.23)–(3.26) for isolated values of A.

6.2. Forward self-similarity

When a backward similarity solution exists, as described in Section 6.1, it is a candidate for describing the local behaviour as the relevant type of singularity is approached. The immediate post-singularity behaviour is then expected to be a forward similarity solution of the form (1.8) with

$$f(\xi) \sim A\xi^\alpha \qquad \text{as} \quad \xi \to +\infty, \tag{6.1}$$
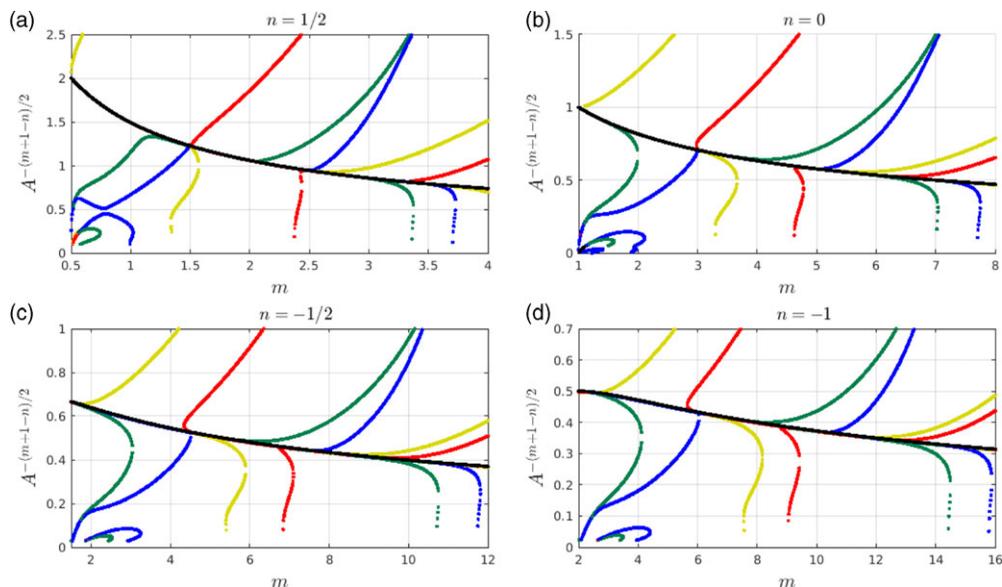
Figure 7. *Locations of viable solutions to the self-similar ODE for (3.21). The exceptional trajectory is indicated by the presence of a black dot. Advancing and receding interface solutions satisfying (3.23) and (3.24) are indicated by red and blue dots, respectively. A touchdown candidate with the near-field behaviour (3.25) is indicated by a green dot, and a leaking candidate, satisfying (3.26), is indicated by a yellow dot.*

where the admissible values of A are determined by the pre-singularity backward solution; (6.1) is supplemented by the relevant boundary conditions at the interface. Importantly, the forward problem is not of eigenvalue type: in contrast to (1.7), an exponentially decaying correction to (6.1) is available and can be constructed by the Liouville-Green method, so the boundary value problem is correctly specified for given A, rather than the possible A being determined as part of the solution (the corresponding quantity then being exponentially growing rather than decaying). It was proved in Corollary 4.2 of [6] that reversing and anti-reversing solutions emanating from suitable behaviour at finite ξ all reach (6.1), for some value of the parameter A, when integrated in the direction of increasing ξ. Associated numerical results are shown in Figure 8, for $n = 0$, $m = 2, 3, 4$, the ODE being solved in the direction of increasing ξ, the approach confirming that arbitrary $A > 0$ can be attained in this fashion.

7. Specific singular phenomena

7.1. Preliminaries

We shall exploit the x and t translation invariance of (1.1) to locate the singularity at $x = 0$ and $t = 0$, without loss of generality (in particular, where a fixed boundary is involved, this will be taken to be at $x = 0$). These symmetries will play further important roles in what follows.

Section 5 gives a detailed description of the two relevant linearisations in terms of special functions. Here we summarise the results in more informal terms and in a self-contained fashion to highlight the information we shall need in the rest of the section. Firstly, the linearisation (5.1) about the spatially uniform solution

$$h = ((1 - n)(-t))^{\frac{1}{1-n}}, \tag{7.1}$$
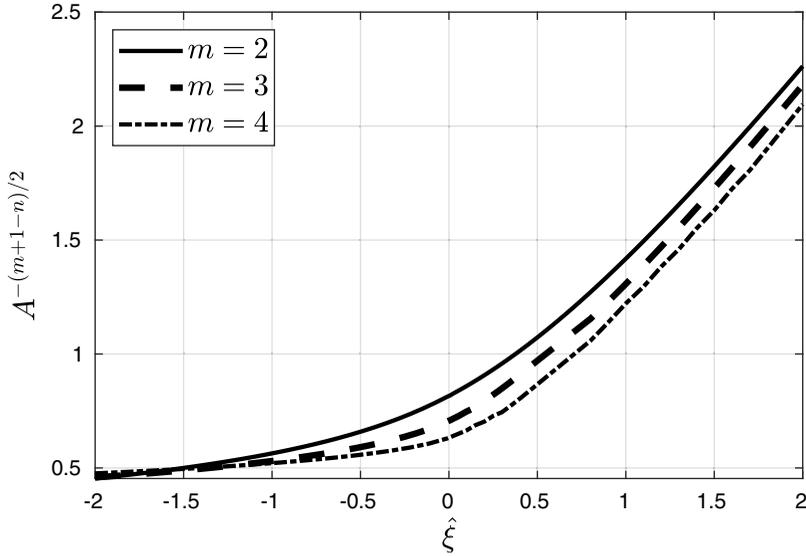
Figure 8. *The connection problem for the self-similar ODE for t > 0; illustrating that connections can be made to arbitrary positive values of A (viable reversers have $A < A_*$ and viable anti-reversers have $A > A_*$).*

leads to the linear PDE (5.2). The relevant backward similarity solutions to this PDE take the form

$$\mathcal{H}_M = (-t)^{\frac{n}{1-n}}(-t)^{\frac{(m+1-n)M}{2(1-n)}}\Psi_M(\eta), \quad \eta = \sqrt{\frac{m+1-n}{2}}(1-n)^{-\frac{(m+1-n)}{2(1-n)}}\frac{x}{(-t)^{\frac{(m+1-n)}{2(1-n)}}}, \quad (7.2)$$

for non-negative integer M, Ψ_M being an Mth order polynomial in η that satisfies

$$-M\Psi_M + \eta\frac{d\Psi_M}{d\eta} = \frac{d^2\Psi_M}{d\eta^2}. \quad (7.3)$$

We normalise $\Psi_M(\eta)$ by requiring that

$$\Psi_M \sim \eta^M \quad \text{as} \quad |\eta| \to \infty, \quad (7.4)$$

so that

$$\Psi_0 = 1, \quad \Psi_1 = \eta, \quad \Psi_2 = \eta^2 - 1, \quad \Psi_3 = \eta^3 - 3\eta, \quad \Psi_4 = \eta^4 - 6\eta^2 + 3. \quad (7.5)$$

The coefficients in Ψ_M alternate in sign, so that the constant term in Ψ_{2N} has the same sign as $(-1)^N$, as does the linear term in Ψ_{2N+1}, an observation that will be relevant in due course. In view of the power of $(-t)$ in the prefactor in (7.2), self-consistency, in the sense that the second term in (5.1) is much smaller than the first in the limit $t \to 0^-$, requires

$$mM + (1-n)(M-2) > 0, \quad (7.6)$$

which is automatically satisfied for $M \geq 1$ in the range of interest here but fails for $M = 0$; the full complement of M is required to furnish a complete set of eigenfunctions to (5.2), an issue to which we shall also implicitly need to return.

Similar issues arise for the linearisation about the steady state

$$h = A_*x^{\frac{2}{m+1-n}}, \quad (7.7)$$

for which $\bar{\mathcal{H}}$, the perturbation about (7.7), satisfies the linear PDE (5.10), which is more conveniently written in the form

$$\frac{\partial \bar{\mathcal{H}}}{\partial t} = A_*^m \left(\frac{\partial^2}{\partial x^2} \left(x^{\frac{2m}{m+1-n}} \bar{\mathcal{H}} \right) - \left(\frac{2n(m+n+1)}{(m+1-n)^2} \right) x^{-\frac{2(1-n)}{m+1-n}} \bar{\mathcal{H}} \right). \tag{7.8}$$

Since we limit ourselves to the range $m + 3n + 1 > 0$, the required backward self-similar solutions to (5.10) (*i.e.* those with maximal regularity as $\eta \to 0^+$, this being a requirement for the subsequent matching) take the form

$$\bar{\mathcal{H}}_M = (-t)^{\frac{n+1-m}{2(1-n)}} (-t)^M \eta^{\frac{n+1-m}{m+1-n}} \Theta_M(\eta), \qquad \eta = A_*^{-\frac{m(m+1-n)}{2(1-n)}} x(-t)^{-\frac{m+1-n}{2(1-n)}}, \tag{7.9}$$

where $\Theta_M(\eta)$ is a polynomial in $\eta^{\frac{2(1-n)}{m+1-n}}$ of Mth order, with

$$-M\Theta_M + \frac{m+1-n}{2(1-n)} \eta \frac{d\Theta_M}{d\eta} = \eta^{-\frac{n+1-m}{m+1-n}} \frac{d^2}{d\eta^2} \left(\eta^{\frac{m+1+n}{m+1-n}} \Theta_M \right) - \frac{2n(m+1+n)}{(m+1-n)^2} \eta^{-\frac{2(1-n)}{m+1-n}} \Theta_M. \tag{7.10}$$

We note that η in (7.9) has the same time dependence as in (7.2), being that of the full similarity solution of Section 6.1, though the constant factor for convenience differs. We normalise $\Theta_M(\eta)$ according to

$$\Theta_M \sim \eta^{\frac{2(1-n)M}{m+1-n}} \qquad \text{as} \quad \eta \to +\infty; \tag{7.11}$$

the coefficients again alternate sign, so that $\Theta_M(0)$ has the same sign as $(-1)^M$; in contrast to Ψ_M, for which the polynomials are alternately odd and even, Θ_M contains all the relevant powers. It follows that

$$\Theta_0 = 1, \qquad \Theta_1 = \eta^{\frac{2(1-n)}{m+1-n}} - 2\frac{(1-n)(n+m+3)}{(m+1-n)^2}, \tag{7.12}$$

$$\Theta_2 = \eta^{\frac{4(1-n)}{m+1-n}} - 4\frac{(1-n)(m+5-n)}{(m+1-n)^2} \eta^{\frac{2(1-n)}{m+1-n}} + 4\frac{(1-n)^2(m+5-n)(n+m+3)}{(m+1-n)^4}. \tag{7.13}$$

Given that (7.7) is proportional to $(-t)^{1/(1-n)}$ for $\eta = O(1)$, self-consistency of (7.9) requires that

$$m < (2M - 1)(1 - n) \tag{7.14}$$

7.2. Extinction behaviour

We start with this case because it involves only one class of self-similar solutions (these being those of the limit problem in Section 4.2, rather than those of the full PDE) and does not involve any post-singular behaviour, h being identically zero following extinction; moreover, it illustrates some principles that will be of more general relevance. We refer to [13] for a very closely related approach to this case.

The extinction behaviour is 'flat' in the sense that it is selected by the linearisation (5.1), with M even in (7.2); in other words, we have 'inner' expansion

$$h \sim ((1-n)(-t))^{\frac{1}{1-n}} - a_N(-t)^{\frac{n+(m+1-n)N}{1-n}} \Psi_{2N}(\eta), , \tag{7.15}$$

with $N \geq 1$ and where a_N is an arbitrary constant that is required to be positive in view of the matching to b_N noted below. In view of (7.4), the expression (7.15) disorders for $|x| \geq O((-t)^{\frac{1}{2N}})$ (*i.e.* the final 'linearised' term in (7.15) becomes comparable with the leading $((1-n)(-t))^{\frac{1}{1-n}}$ term). On this outer scale, the dominant balance in (1.1) is given by

$$\frac{\partial h}{\partial t} \sim -h^n$$

so that (*cf.* Section 4.2)

$$h \sim (-t)^{\frac{1}{1-n}} \left((1-n) \left(1 - b_N \frac{x^{2N}}{(-t)} \right) \right)^{\frac{1}{1-n}} \tag{7.16}$$

with $b_N \propto a_N$; the matching condition ('inner of outer') that follows from (7.16) can readily be inferred. From (7.16) it follows that the interfaces satisfy

$$x \sim \pm \left(\frac{(-t)}{b_N} \right)^{\frac{1}{2N}} \qquad \text{as} \quad t \to 0^-,$$

wherein b_N is an arbitrary positive constant.

We now discuss the status of N in the analysis above in terms of the stability (reflecting the completeness of the eigenfunctions) and of the necessity for an entire family of possible asymptotic behaviours (N being an arbitrary positive integer). The case $N = 1$ is expected to provide the generic (*i.e.* stable) extinction behaviour; while the solution to (5.2) will in general also contain $\mathcal{H}_0$ and $\mathcal{H}_1$ contributions, each of these being eliminated by identifying $x = 0$, $t = 0$ with the place and time of extinction (it is no coincidence that there are two translation symmetries and that two eigenfunctions need to be suppressed); indeed, $\mathcal{H}_0$ corresponds to a small shift in t in (1.6), while $\mathcal{H}_M \propto \partial \mathcal{H}_{M+1}/\partial x$, so an x translation in $\mathcal{H}_2$ can suppress $\mathcal{H}_1$. Similar arguments apply in the singular scenarios outlined below, where we typically omit such details (see the end of Section 5.2, however). The necessity for the non-generic cases $N \geq 2$ can be argued as follows: for initial data containing a minimum between the two maxima, two generic behaviours can occur prior to extinction:

1. diffusion may eliminate the minimum to leave a single maximum or
2. the sink term may lead to the minimum touching down (as described in the next subsection), with the support of h breaking into two disconnected sets.

The case $N = 2$ (which has a minimum at $\eta = 0$) describes intermediate-asymptotic behaviour on the borderline between these two, with yet higher N corresponding to borderlines between scenarios that are themselves non-generic (the inevitability of the latter being implicit in the above identification of the necessity of a scenario with $N = 2$, enabling a bootstrapping argument to higher and higher N given the presence of the comparable families associated with other types of singular behaviour).

In summary, as well as characterising a particularly significant type of intermediate-asymptotic behaviour, the above illustrates a central element of the subsequent subsections, namely the existence of a (discrete) set of asymptotic possibilities, the leading one of which is generic, this being particularly transparent in the current case given that the relevant solution to the heat equation can be written as a sum over the Hermite polynomials (5.5) with $k \geq 2$. The number of modes to which a given asymptotic scenario is unstable is readily identified from such a representation in terms of the omitted contributions and the non-generic behaviours play an identifiable role in the dynamics: for example, and as noted above, the case $C_2 = C_3 = 0$ can be interpreted as providing the borderline between solutions whose support breaks up prior to extinction and those for which it does not.

7.3. Touchdown

It is noteworthy that there are three distinct intermediate-asymptotic scenarios in this case. Firstly, the results of the previous subsection can be immediately revisited with the only changes being $a_N \to -a_N$ and $b_N \to -b_N$, with a_N and b_N then still positive. Hence, in particular, (7.16) becomes

$$h \sim (-t)^{\frac{1}{1-n}} \left((1-n) \left(1 + b_N \frac{x^{2N}}{(-t)} \right) \right)^{\frac{1}{1-n}} \tag{7.17}$$

so that the local profile at $t = 0$ is given by

$$h(x, 0) \sim \left((1-n) b_N x^{2N} \right)^{\frac{1}{1-n}} \qquad \text{as} \quad |x| \to 0.$$

For $t \to 0^+$ (*i.e.* after the touchdown and film rupture at $t = 0$), one then has the asymptotic behaviour

$$h \sim \left((1-n) \left(b_N x^{2N} - t \right) \right)^{\frac{1}{1-n}} \tag{7.18}$$

with retracting interfaces given by

$$x \sim \pm \left(\frac{t}{b_N} \right)^{\frac{1}{2N}},$$

and with $h \equiv 0$ for smaller $|x|$; since (7.18) is consistent with (2.2), the former needs no supplementation by an inner scaling.

Secondly, the green curves in Figure 7 are of the required type for the pre-touchdown local behaviour, while the associated post-touchdown local behaviour is then expected to be a forward similarity solution of the form (1.7).

Thirdly, and clarifying the bifurcation structure in Figure 7, the black branch therein, which gives the exceptional solution, can be followed in the sense of the linearisation (5.10), so that

$$h \sim \begin{cases} A_* x^{\frac{2}{m+1-n}} + c_M^+ \bar{\mathcal{H}}_M(x, t) & \text{for} \quad \eta > 0, \\ A_*(-x)^{\frac{2}{m+1-n}} + c_M^- \bar{\mathcal{H}}_M(-x, t) & \text{for} \quad \eta < 0, \end{cases} \tag{7.19}$$

provides the outer (*i.e.* $\eta = O(1)$) expansion, with arbitrary constants $c_M^\pm$ and $\bar{\mathcal{H}}_M$ and η as in (7.9). Here, the pre-touchdown solution of Section 3.1, see (3.8), comes into play via its quasi-steady generalisation: the resulting inner scalings are

$$x = (-t)^M \xi, \qquad h = (-t)^{\frac{2M}{m+1-n}} g(\xi) \tag{7.20}$$

implying the quasi-steady balance (as in Section 3.1)

$$\frac{d}{d\xi} \left(g^m \frac{dg}{d\xi} \right) \sim g^n \tag{7.21}$$

at leading order. The matching condition

$$g \sim A_* |\xi|^{\frac{2}{m+1-n}} \qquad \text{as} \quad |\xi| \to \infty \tag{7.22}$$

specifies the solution to (7.21) up to arbitrary constants ξ_0 and α in the form

$$g = \alpha^2 G \left(\frac{\xi + \xi_0}{\alpha^{m+1-n}} \right) \tag{7.23}$$

where $G(\sigma)$ is an even function of σ that can be specified uniquely via

$$G(\sigma) \sim A_* \sigma^{\frac{2}{m+1-n}} + \sigma^{\frac{n+1-m}{m+1-n}} \qquad \text{as} \quad \sigma \to +\infty \qquad \text{for} \quad n > 0,$$

$$G(\sigma) \sim A_* \sigma^{\frac{2}{m+1-n}} - \sigma^{\frac{n+1-m}{m+1-n}} \qquad \text{as} \quad \sigma \to +\infty \qquad \text{for} \quad n < 0, \tag{7.24}$$

The switch in sign follows (as in (3.10) above) from an analysis of the integral that arises on solving the separable equation

$$\frac{1}{2} G^{2m} \left(\frac{dG}{d\sigma} \right)^2 - \frac{1}{m+n+1} \left(G^{m+n+1} - G_0^{m+n+1} \right) = 0$$

that results as the first integral of (7.21), where

$$G_0 = G(0).$$

In the special case $n = 0$ already noted above, we have

$$G = \left(G_0 + \frac{m+1}{2} \sigma^2 \right)^{\frac{1}{m+1}}$$

and the correction terms in (7.24) are instead absent; we omit further analysis of this exceptional case here.

Given that

$$\bar{\mathcal{H}}_M \sim K_M(-1)^M(-t)^M x^{\frac{n+1-m}{m+1-n}} \qquad \text{as} \quad \eta \to 0. \tag{7.25}$$

for some positive constant K_M that is to be regarded as known, given the analysis of Section 5.2, matching to (7.20) and (7.24) implies that α and ξ_0 are given by

$$\frac{2}{m+1-n}\xi_0 A_* \pm \alpha^{m+1-n} = (-1)^M c_M^+ K_M$$

$$-\frac{2}{m+1-n}\xi_0 A_* \pm \alpha^{m+1-n} = (-1)^M c_M^- K_M \tag{7.26}$$

where the signs on the left-hand sides correspond to those in (7.24). Self-consistency of such a scenario requires that (7.14) hold. Before turning to questions of stability, it is helpful to make connections between (7.26) and Figure 7; the green branches in the latter bifurcate off when equality holds in (7.14) and are symmetric. For m slightly larger than $(2M-1)(1-n)$, the expressions (7.26) remain relevant with $\xi_0 = 0$, $c_M^+ = c_M^- = c_M$; since α is necessarily positive (a constraint with broader implications in (7.26)), this implies $c_M > 0$ and hence $A > A_*$ for $n < 0$, M odd and $n > 0$, M even, with $c_M < 0$ and $A < A_*$ in the converse cases. This is consistent both with the alternating directions of the green branches in Figure 7 and with their swapping sides as n passes through zero. Turning now to stability, $N = 1$ in (7.17) leads to a generic cases, as in the previous subsection; $N \geq 2$ scenarios are again necessary but unstable. We signpost that the cases akin to (7.17), but with M odd, will also be relevant in due course. In terms of (7.19), the cases $\eta > 0$ and $\eta < 0$ in effect operate independently, so suppressing the $M = 0$ mode in (5.10) on both sides uses up both translational invariants. Since (7.14) is violated for $M = 1$, $m + n > 1$, the first legitimate instance of (7.19) is doubly unstable (though in the symmetric case, or with zero-Neumann boundary condition on $x = 0$ (for which x translational invariance cannot be exploited), it is only singly so). However, for related reasons the left-most green branch in panel of Figure 7 with $n \leq 0$ is expected to be stable[4] above the fold, but unstable below it: in these regimes there are thus two stable scenarios, that in Figure 7 for a narrow range of $m > 1 - n$, while (7.17) with $N = 1$ is applicable throughout. In Figure 7, successive branches (of any colour) are expected to gain an additional unstable mode on each occasion a bifurcation point is passed through from left to right.

At $t = 0$, the spatial profiles in the third scenario take the form

$$h \sim A_*|x|^{\frac{2}{m+1-n}} + c_M^\pm |x|^{\frac{n+1-m+2M(1-n)}{m+1-n}} \qquad \text{as} \quad |x| \to 0. \tag{7.27}$$

There seems subsequently to be the possibility of non-uniqueness, but we shall not discuss the associated post-touchdown behaviour given that these are in any case unstable.

7.4. Attachment, detachment and coalescence

Attachment, either to a fixed boundary or through two interfaces colliding (either through both advancing or by one advancing faster than the other is retracting) – termed coalescence above – raises no presingularity questions since the solution has no prior knowledge that it is about to attach (unlike the other cases analysed here).[5] Post-attachment raises no significant challenges either: one has a porous-medium equation similarity solution of the form

$$h \sim t^{\frac{1}{m}} f\left(\frac{x}{t}\right) \qquad \text{as} \quad \text{with} \quad x = O(t),$$

---

[4]For $n > 0$, the corresponding branch is anticipated to lie in $m + n < 1$.

[5]We note that here we are assuming that $\dot{s}(0) \neq 0$. For the porous-medium equation waiting-time behaviour, $\dot{s} \equiv 0$ can occur for small enough times but the interface must subsequently advance at finite speed for all t; we shall not explore such phenomena here – see [21] and [20] for such behaviour in the porous-medium equation.

with additional structure when an advancing interface overuns a receding one of a form akin to that analysed in the generic anti-reverser case addressed below. One related observation is in order; however, the pre-attaching behaviour of an advancing interface takes the form

$$h \sim (-t)^{\frac{1}{m}} f\left(\frac{x}{(-t)}\right), \qquad f^m(\eta) = m\eta_0(\eta_0 - \eta)$$

for some constant η_0. This simply corresponds to a Taylor expansion in t of (2.3), reflecting the lack of prior knowledge referred to above, but is also an exceptional connection for the porous-medium equation in a sense elaborated upon in [14], the significance of which here is that this relates to the probably unexpected branches present in the bottom left-hand corners of Figure 7, though we shall not go into details here.

There are of course non-generic attaching behaviours, such as an interface reversing at the same instant as attaching, but the no-prior-knowledge argument applies to these also. For the hole filling case in higher dimensions, the situation is more complicated, however, since the interface is aware of its increasing curvature; see, for example, [1] for the porous-medium equation – including a sink term, as in (1.1), leads to open questions in this regard.

The detachment case is also simple in the sense that we conjecture that the left-most yellow branch in each panel of Figure 7 provides the generic behaviour, with post-detachment being described by an associated forward similarity solution. For $n > 0$, we expect this branch to start from $A < A_*$ as $m + n \to 1^+$ (with a fold in $m + n < 1$ connecting the branch to $A = A_*$ at $m + n = 1$), whereas for $n \leq 0$ we have $A \to A_*$ in that limit. Non-generic cases arise both as the other yellow branches and from tracking along the black branch prior to the secondary and subsequent bifurcations, as in the first of (7.19), being subject to (7.14). Now a quasi-steady version of the leaking solution of Section 3.1, satisfying (3.6), describes the inner behaviour – the inner scalings are again given by (7.20), but now (7.21) is subject to

$$g = 0 \qquad \text{at} \quad \xi = 0$$

so that

$$g = \alpha^2 G\left(\frac{\xi}{\alpha^{m+n-1}}\right)$$

with

$$\frac{1}{2}G^{2m}\left(\frac{dG}{d\sigma}\right)^2 - \frac{1}{m+1}G^{m+n+1} = \frac{1}{2}J_0^2$$

where

$$J_0 = G^m \frac{dG}{d\sigma}\bigg|_{\sigma=0} > 0$$

determines the outward flux. For $n = 0$, we have

$$G = \left((m+1)\left(J_0\sigma + \frac{1}{2}\sigma^2\right)\right)^{\frac{1}{m+1}}$$

and for any n the sign in the first of (7.24) applies here – correspondingly, the yellow branches of Figure 7 are on the opposite sides from the green ones for $n < 0$ and on the same side for $N > 0$. The local behaviour at detachment is then again as in (7.27). Instability follows even for $M = 2$ because the x-translation mode is not available given the boundary condition (*i.e.* $h = 0$ at $x = 0$), and the $M = 0$ and $M = 1$ modes both need to be absent; accordingly, we omit any discussion of the post-detachment behaviour in these non-generic cases.

7.5. Reversers and anti-reversers

We start with scenarios in which the two have closely related behaviour, before discussing a (generic) anti-reversing structure distinct from the other categories arising here. We take the support to lie in $x > 0$ at $t = 0$ and start from the first of (7.19) (writing $c_M = c_M^+$) with, as always, (7.14) being required. Since here we can apply both t and x translational invariance, the $M = 0$ and $M = 1$ modes can both be suppressed (in contrast to the situation in the previous section), leaving $M = 2$ as a potential stable scenario for $m < 3(1 - n)$. The matching condition

$$h \sim A_* x^{\frac{2}{m+1-n}} + (-1)^M K_M c_M (-t)^M x^{\frac{n+1-m}{m+1-n}} \tag{7.28}$$

then applies on a travelling-wave inner region, for which a translation

$$x = s(t) + z, \qquad s(t) \sim \frac{(-1)^{M+1} K_M c_M}{A_*} (-t)^M \tag{7.29}$$

is required, with the dominant balance being (as in Section 3.2)

$$-\dot{s} \frac{\partial h}{\partial z} \sim \frac{\partial}{\partial z} \left(h^m \frac{\partial h}{\partial z} \right) - h^n, \tag{7.30}$$

which implies that the inner scalings are

$$z = O\left((-t)^{\frac{(m+1-n)(M+1)}{m+n-1}} \right), \qquad h = O\left((-t)^{\frac{2(M-1)}{m+n-1}} \right). \tag{7.31}$$

Given that the outer scaling associated with (7.19) is the full self-similar one, $x = O\left((-t)^{\frac{m+1-n}{2(1-n)}} \right)$, consistency conditions on the above read

$$\frac{(m+1-n)(M-1)}{m+n-1} > M > \frac{m+1-n}{2(1-n)}, \tag{7.32}$$

both inequalities simply reproducing (7.14). Whether (7.28) is associated with a reverser or an anti-reverser depends upon the sign of c_M; if $c_M(-1)^{M+1}$ is positive the above asymptotic behaviour corresponds to a reverser (advancing interface for $t < 0$), while if it is negative it is an anti-reverser (receding interface for $t < 0$),[6] subject to the following qualification – for the stable case $M = 2$ and other even M the interface indeed changes direction (see (7.29)), while for M odd it recommences its original direction after an instantaneous pause (the singly unstable case $M = 3$ corresponding to the borderline between (i) reversers and anti-reversers occurring in rapid succession (in either order) and (ii) no change of direction).

A first integral of (7.30) is available in the case $n = 0$, namely

$$-\dot{s} h = h^m \frac{\partial h}{\partial z} - z.$$

With regard to the transcritical red/blue bifurcations in Figure 7, for $n < 0$ the numerics provide evidence that the primary such bifurcation has red unstable and blue stable close to the bifurcation point, though with folds rapidly swapping the stability of each, whereas for $n > 0$ the red branch is expected to be stable throughout and the blue unstable (except perhaps in the lower left-hand corner: we leave the stability of the branches there as an open question). Similar comments apply with respect to the number of unstable model arising from the subsequent bifurcations.

Collecting together the implications of the above for the generic cases, we summarise our conjectures as follows.

---

[6]The presence of the $(-1)^{M+1}$ here is reflected in the red and blue branches repeatedly swapping sides in Figure 7.

(I) Reversers

For $m < 3(1 - n)$, (7.28)–(7.30) with $M = 2$ provide a stable solution, changing direction smoothly (*i.e.* $s \propto (-t)^2$ in (7.29)). At $t = 0$

$$h \sim A_* x^{\frac{2}{m+1-n}} + \kappa x^{\frac{5-3n-m}{m+1-n}} \tag{7.33}$$

holds for some constant κ and the $t \to 0^+$ behaviour follows directly from the $t \to 0^-$ behaviour (the equivalent polynomial solutions provide the correction term, though their coefficients then all take the same sign). For $n > 0$, the generic behaviour in $m > 3(1 - n)$ is a full similarity solution, corresponding to the first red branch in Figure 7. For $n < 0$, the situation is slightly more complicated, with a bistable regime being present over a small range of m in $m < 3(1 - n)$, the red branch being unstable below the fold (being the borderline between the two stable scenarios) but stable above it and continuing into the range $m > 3(1 - n)$. When a full similarity solution applies, s is in general not smooth:

$$s \sim S_-(-t)^{\frac{m+1-n}{2(1-n)}} \quad \text{as} \quad t \to 0^-, \qquad s \sim S_+ t^{\frac{m+1-n}{2(1-n)}} \quad \text{as} \quad t \to 0^+, \tag{7.34}$$

with a forward similarity solution holding as $t \to 0^+$ and with the constants S_- and S_+ presumably being different and positive on the primary branch.

(II) Anti-reversers

The description in (I) above again applies for $m < 3(1 - n)$, $M = 2$ (whether a reverser or anti-reverser pertains depends on the sign of κ). For $n < 0$ there is expected to be a narrow range of bistability in $m > 3(1 - n)$ also (one of the stable scenarios being the full similarity solution, as in Figure 7, the other being described next), but the first blue branch is otherwise unstable, necessitating the identification of a different class of intermediate-asymptotic behaviour. The range $m < 3(1 - n)$ is thus bistable, with the blue branch expected to provide the borderline between the two generic cases.

An important clue into the other generic scenario is provided by a comparison between (2.2) and (2.3): since

$$1 - n < m \quad \text{for} \quad m + n > 1,$$

retreating interfaces are associated with local behaviour smaller than that of the advancing ones, so we may anticipate that the latter can overrun the former with little modification to itself. We now formalise that intuition; related analyses of the porous-medium equation, [19, 20], represent precedents. Two outer regions are present on the scaling $x = O(-t)$, namely

$$\begin{aligned} h^m &\sim mq(x - q(-t)) & \text{for} \quad \frac{x}{(-t)} > q, \\ h^{1-n} &\sim (1 - n)\left(-t + \frac{x}{Q}\right) & \text{for} \quad q > \frac{x}{(-t)} > -Q, \end{aligned} \tag{7.35}$$

wherein q and Q are each positive constants, the former expression being a similarity solution of the porous-medium equation (as in Section 4.1) and the latter being one of the pure absorption limit (as in Section 4.2). The two expressions in (7.35) are comparable for

$$x = q(-t) + O\left((-t)^{\frac{m}{1-n}}\right),$$

self-consistency here again requiring that $m + n > 1$, which implies the inner scalings

$$x = q(-t) + (-t)^{\frac{m}{1-n}} \xi, \qquad h = (-t)^{\frac{1}{1-n}} g,$$

leading to

$$q \frac{\partial g}{\partial \xi} \sim \frac{\partial}{\partial \xi}\left(g^m \frac{\partial g}{\partial \xi}\right)$$

and hence to

$$q\left(g - \left((1-n)\left(1 + \frac{q}{Q}\right)\right)^{\frac{1}{1-n}}\right) \sim g^m \frac{\partial g}{\partial \xi},$$

thereby matching with (7.35) in both limits $|\xi| \to \infty$. In consequence, we simply have

$$h(x, 0) \sim (mqx)^{\frac{1}{m}} \qquad \text{as} \quad x \to 0^+$$

so the interface obeys

$$x \sim Qt \quad \text{as} \quad t \to 0^-, \qquad x \sim -qt \quad \text{as} \quad t \to 0^+, \tag{7.36}$$

its velocity being discontinuous (indeed swapping sign) at $t = 0$.

There is one final, but unstable, case to which we have already alluded and for which relevant results can be read off directly from (7.17) on replacing the even exponent by an odd one, so that

$$h \sim (-t)^{\frac{1}{1-n}} \left((1-n)\left(1 + b_N \frac{x^{2N+1}}{(-t)}\right)\right)^{\frac{1}{1-n}}$$

with $N \geq 1$ and with $b_N > 0$ without loss of generality. This has a retreating interface for $t < 0$ at

$$x \sim -\left(\frac{(-t)}{b_N}\right)^{\frac{1}{2N+1}},$$

with $h \equiv 0$ for smaller x, and

$$h(x, 0) \sim \left((1-n)b_N x^{2N+1}\right)^{\frac{1}{1-n}} \qquad \text{as} \quad x \to 0^+.$$

Since the interface has

$$x \sim \left(\frac{t}{b_N}\right)^{\frac{1}{2N+1}} \qquad \text{as} \quad t \to 0^+$$

in this case, no change of direction occurs, with $N = 1$ being singly unstable and providing the borderline between solutions that lose a local maximum/minimum pair while retreating and those which touchdown. These cases are striking in having unbounded, rather than zero, interface velocity at $t = 0$ and do not fall naturally under any of the headings above.

8. Numerical solutions to the PDE

8.1. Validation of the asymptotic predictions

Here we provide evidence to substantiate the observability of some of the local descriptions identified as generic above. First, we summarise the findings of the numerical experiments, and then, we give the details on how solutions to (1.1) were found by direct numerical simulation. All results in this section have $n = 0$ but similarly good agreement is expected for other values of n in the range (1.2).

(i) Reversing events. Panel (ia) in Figure 9 indicates that for $m < 3(1 - n)$ we have $s \sim \text{const.}(-t)^2$ as $t \to 0^-$ with the constant dependent upon the initial conditions. This is in agreement with (7.33). Panel (ib) indicates that for $m > 3(1 - n)$ we have $s \sim \hat{\xi}(-t)^{(m+1-n)/2(1-n)}$ where the constant $\hat{\xi}$ is that obtained from the ODE solutions described in Section 6 on the stable red branch: we find

$$\hat{\xi} \approx 0.3864 \quad \text{for} \quad m = 4, \quad n = 0, \tag{8.1}$$

$$\hat{\xi} \approx 0.5014 \quad \text{for} \quad m = 5, \quad n = 0, \tag{8.2}$$

the PDE simulations being consistent with these values up to three significant figures.
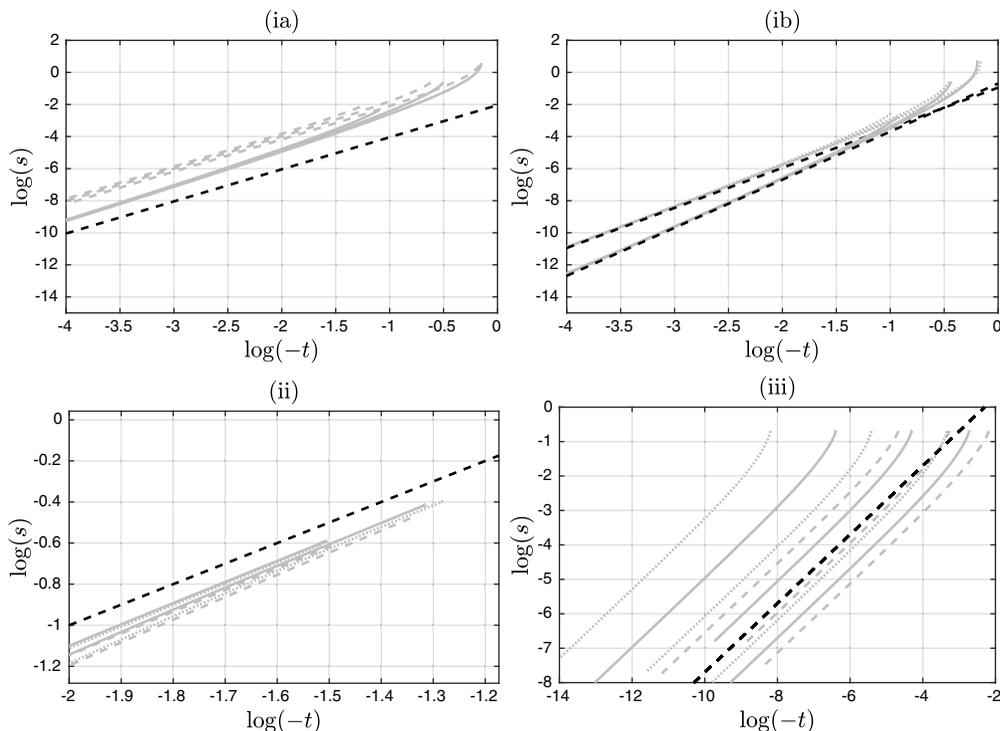
Figure 9. *Comparison between the asymptotic results, shown in grey, and direct numerical simulation of (1.1), shown in black, for n = 0. Panels (ia) and (ib) show the interface position leading up to a reversing event for different choices of initial condition. In (ia) dashed curves are for m = 2, whereas solid ones are m = 3. In (ib), dotted curves are for m = 4 and solid curves for m = 5. Panels (ii) and (iii) show the interface position leading up to anti-reversing and attachment events, respectively, for different choices of initial condition. In both panels (ii) and (iii), dashed curves indicate m = 2, solid curves m = 3 and dotted curves m = 4.*

(ii) Anti-reversing events.   Panel (ii) in Figure 9 indicates that the interface obeys $s \sim \text{const.}(-t)$ with the constant selected by the initial data, in agreement with (7.36). We omit here the other regime of stable anti-reversing identified in Section 7.5, namely pure self-similarity.

(iii) Attaching events.   Panel (iii) in Figure 9 indicates that the interface obeys $s \sim \text{const.}(-t)$ with the constant selected by the initial data in agreement with the discussion in Section 7.4; in short, this is expected because the interface has no way to anticipate its collision with the absorbing boundary.

(iv) Detaching events.   Panel (iv) in Figure 10 indicates that the outward flux at the interface leading up to a detachment event obeys

$$h^m \frac{\partial h}{\partial x}\bigg|_{x=0} = (-t)^{(m+1)/2} f^m \frac{\partial f}{\partial \xi}\bigg|_{\xi=0} \tag{8.3}$$

where the quantity $f^m \partial f / \partial \xi|_{\xi=0}$ can be determined via the shooting method described in Section 6. Shooting on the self-similar ODE yields

$$f^m \frac{\partial f}{\partial \xi}\bigg|_{\xi=0} = 0.4912 \quad \text{for} \quad m=2, \quad n=0, \tag{8.4}$$
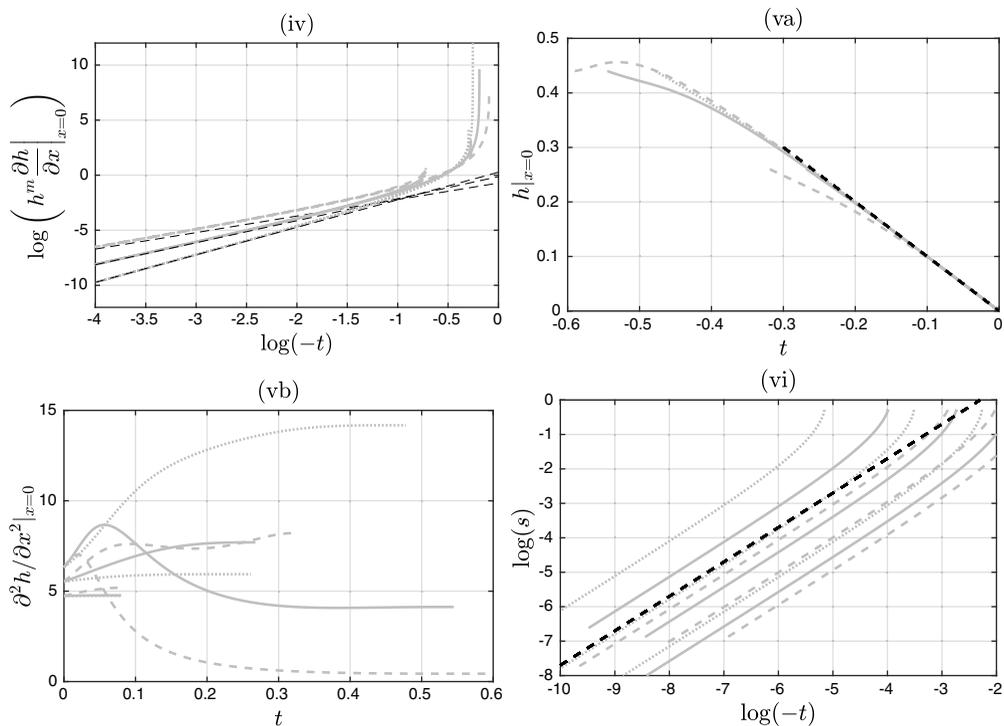
Figure 10. *Comparison between the asymptotic results, shown in grey, and direct numerical simulation of (1.1), shown in black, for $n = 0$; results for $m = 2$ are indicated by dashed curves, for $m = 3$ with solid curves and for $m = 4$ with dotted curves. Panel (iv) shows the flux at the interface leading up to a detachment event for different choices of initial condition. Panels (va) and (vb) show h and h_{xx} at the minimum leading up to a touchdown event.*

$$f^m \frac{\partial f}{\partial \xi}\bigg|_{\xi=0} = 0.8786 \quad \text{for} \quad m = 3, \quad n = 0, \tag{8.5}$$

$$f^m \frac{\partial f}{\partial \xi}\bigg|_{\xi=0} = 1.3076 \quad \text{for} \quad m = 4, \quad n = 0, \tag{8.6}$$

with which the PDE solutions are again consistent up to three significant figures. This verifies the claim in Section 7.4 that the left-most yellow branch in Figure 7 provides the generic description of detachment.

(v) Touchdown events. Panels (va) and (vb) in Figure 10 indicate that the description leading up to a touchdown event are in agreement with (7.18) with $N = 1$, verifying that this is the generic behaviour; we note that the curvature does not tend to a constant at $t \to 0^-$ in cases where $N > 1$.

(vi) Coalescence events. Panel (vi) in Figure 10 indicates that the interfaces obey $s \sim \text{const.}(-t)$ with the constant selected by the initial data, in agreement with the discussion in Section 7.4 and again following from the no-prior-knowledge argument.

8.2. Numerical methods

We furnish numerical solutions (1.1) on a finite domain by supplementing it with an interface condition at the left-hand end of its compact support, that is, one of the conditions (1.3)–(1.5), as well as a symmetry condition at some location $x = x_0 > 0$, that is,

$$\left.\frac{\partial h}{\partial x}\right|_{x=x_0} = 0. \tag{8.7}$$

The value of x_0 is chosen arbitrarily; the spatial coordinates are translated post hoc such that the singular event occurs at $x = 0$.

Numerical solution is made awkward by two features, namely (a) that the domain is dynamic and (b) that the solution often exhibits an infinite spatial gradient at the interface. We alleviate these difficulties by transforming the spatial coordinates using a similar strategy to that in [6]. As we have seen, the solution local to an interface takes the form

$$h \sim \lambda(t)(x - s(t))^\omega \quad \text{as} \quad x \to s(t)^+ \tag{8.8}$$

for some λ, where $\omega = 1/m, 1/(1-n), 1/(m+1)$ or $2/(m+1-n)$ depending on whether the interface is advancing, receding, in contact with an absorbing boundary or stationary and mass preserving. These local behaviours motivate the coordinate transformations

$$y = \left(1 - \frac{x_0 - x}{x_0 - s(t)}\right)^\omega \tag{8.9}$$

such that the behaviour (8.8) is replaced with $h \sim \hat{\lambda}(t)y$ as $y \to 0^+$. The PDE (1.1) becomes

$$\frac{\partial h}{\partial t} = \frac{wy^{(w-1)/w}}{x_0 - s} \frac{\partial}{\partial y}\left(\frac{wy^{(w-1)/w}}{x_0 - s}h^m \frac{\partial h}{\partial y}\right) + \frac{w\left(1 - y^{1/w}\right)y^{(w-1)/w}}{x_0 - s} \frac{ds}{dt}\frac{\partial h}{\partial y} - h^n. \tag{8.10}$$

This is closed by the boundary conditions

$$h|_{y=0} = 0, \quad \left.\frac{\partial h}{\partial y}\right|_{y=1} = 0, \tag{8.11}$$

where the latter results from transforming (8.7) and the former results from (1.3a) for a mobile interface or (1.5) for an absorbing boundary. When an absorbing boundary is being considered we have $\dot{s} = 0$, but for a dynamic interface the motion is solved for as part of the solution to the problem using the transformed counterpart of (1.4), which reads

$$\dot{s} = \lim_{y \searrow 0} \begin{cases} -\dfrac{wy^{(w-1)/w}}{x_0 - s}h^{m-1}\dfrac{\partial h}{\partial y} & \text{if } \dot{s}(t) \leq 0, \\[2ex] \dfrac{h^n(x_0 - s)}{wy^{(w-1)/2}}\left(\dfrac{\partial h}{\partial y}\right)^{-1} & \text{if } \dot{s}(t) \geq 0. \end{cases} \tag{8.12}$$

The spatial derivatives in the PDE (8.10) and the boundary conditions (8.11) (along with (8.12) in scenarios where an interface is moving) are discretised using finite differences. Second-order central differences are used on internal points, while the ghost-point method is used to incorporate (8.11). To retain second-order accuracy, the spatial derivative in (8.12) is computed using a forward-finite-difference approximation involving values of h at the node in question and two neighbouring nodes. Once this has been done, the resulting large system of coupled ODEs is integrated forward in time using an adaptive Runge–Kutta–Fehlberg (RKF45) scheme implemented in MATLAB.

9. Discussion

As will be clear from the lengthy analysis above, the PDE (1.1), despite being deceptively simple looking, displays a wide variety of singular behaviours. We have investigated these using a combination of formal asymptotics and numerical methods, and our results leave open a considerable number of open questions deserving of a rigorous analytical treatment.

We now outline some broader implications of the types of approach implemented here, firstly for singularity development in moving-boundary problems and nonlinear PDEs and secondly for symmetry methods. In the former regard, the classes of phenomena explored here are of broad relevance (in terms

both of the rather comprehensive nature of the transitions summarised by Figure 1 and of the necessity for hierarchies of less and less generic types of singularity formation) for systems in which interfaces can both advance and retreat and in which touchdown can occur. Another well-known such example is that of the thin-film equation, in which touchdown is associated with film rupture; the current example is perhaps the simplest though, being of second order – moreover, retreat and touchdown both become impossible for $n \geq 1$, so (1.1) also serves to illustrate a further type of transition. Two further constraints (namely $m + n > 1$ and $m + 3n + 1 > 0$) have been imposed above – the transitions that occur on passing through these borderlines are less dramatic but nevertheless require that the resulting parameter regimes be afforded separate treatment.

In terms of similarity methods, we focus here on issues associated with the linear stability of the postulated self-similar forms, illustrating more general principles through the current specific application, to which the scaling reduction

$$h = (-t)^{\frac{1}{1-n}} f(\eta), \qquad \eta = \frac{x}{(-t)^{\frac{m+1-n}{2(1-n)}}} \tag{9.1}$$

applies; the two symmetries not used up by (9.1) (i.e. t and x translation invariants) can each be applied to generate solutions that satisfy (1.1) linearised about (9.1), namely

$$\frac{\partial H}{\partial \tau} + \frac{m + 1 - n}{2(1 - n)} \eta \frac{\partial H}{\partial \eta} = \frac{\partial^2}{\partial \eta^2} (f^m H) - n f^{-(1-n)} H, \tag{9.2}$$

where $\tau = -\ln(-t)$. That (9.2) is autonomous in τ (and hence separable) is a remnant of the scaling invariance of (1.1). The solutions to (9.2) resulting from the translation invariants are

$$H = \frac{\partial h}{\partial t} = (-t)^{\frac{n}{1-n}} \left(-f + \frac{m + 1 - n}{2} \eta \frac{df}{d\eta} \right), \tag{9.3}$$

and

$$H = \frac{\partial h}{\partial x} = (-t)^{\frac{n+1-m}{2(1-n)}} \frac{df}{d\eta}. \tag{9.4}$$

Because (9.2) is second-order and linear, so that Sturm-Liouville theory is applicable for suitable boundary data, the number of zeros on each of these provides insight into the stability properties of (9.1); *cf.* [2], for example, for related arguments. In the current context, (9.3) and (9.4) should be regarded as unstable modes, both growing relative to (9.1) as $t \to 0^-$, a result implicit in our translations of x and t to prescribe the singularities to occur at the origin of each.

Central to our analyses have been two special solutions to (1.1), namely

$$h = ((1 - n)(-t))^{\frac{1}{1-n}}, \tag{9.5}$$

and

$$h = A_* x^{\frac{2}{m+1-n}}. \tag{9.6}$$

As already noted, these are exceptional with regard to symmetry methods (being invariant under two distinct symmetries); it is therefore perhaps not surprising that they also play an exceptional role in delineating the possible intermediate-asymptotic properties. Their doubly symmetric nature has implications for the linearisation, an issue which we have touched on above: the linearised equation for $H(x, t)$ is autonomous in x for (9.5) and in t for (9.6) implying successive modes derived in Section 5.1 involve successive integrations with respect to x and those in Section 5.2 successive integrations with respect to t, prefiguring some of the properties that we have exploited and being revisited below. The τ translation invariance of (9.3) also remains significant, however – we recall that each of (9.5) and (9.6) is a special case of (9.1). Moreover, the doubly symmetric attributes of (9.5) and (9.6) have further implications: (9.4) is identically zero for (9.5), as is (9.3) for (9.6), so more needs to be said with regard to the application of the translation invariants, there being significant differences from the roles these play for more general f.

We write the general solution to (9.2) in the form (glossing over boundary conditions and ignoring the role of nonlinearities, neither of which lead to fundamental difficulties)

$$H = \sum_{n=0}^{\infty} A_M(-t)^{\lambda_M} F_M(\eta), \tag{9.7}$$

where $t = -e^{-\tau}$, the $F_M(\eta)$ form a complete set of normalised eigenfunctions, the A_M are arbitrary constants and the λ_M form an increasing sequence. We define $H_M = (-t)^{\lambda_M} F_M(\eta)$. Except for (9.5) and (9.6), when $f(\eta)$ is stable we expect

$$\begin{aligned}
\lambda_0 &= \frac{n+1-m}{2(1-n)}, \quad F_0 = \frac{df}{d\eta}, \\
\lambda_1 &= \frac{n}{1-n}, \qquad F_1 = -f + \frac{m+1-n}{2}\eta\frac{df}{d\eta},
\end{aligned} \tag{9.8}$$

when $m+n > 1$ (that these two swap dominance at $m+n = 1$ is a further indication of the significance of that borderline). In view of (9.3), (9.4), these can (and should, given that they would otherwise dominate (9.1)) be absorbed into $f(\eta)$ by suitable x and t translations, respectively, so that (9.7) is dominated by $M = 2$ (with $\lambda_2 > 1/(1-n)$ when $f(\eta)$ is stable). The situation with (9.5) and (9.6) is more complicated, however. For (9.5) we have

$$\lambda_M = \frac{n}{1-n} + \frac{m+1-n}{2(1-n)}M \tag{9.9}$$

with $F_0 = 1$, $dF_{M+1}/d\eta = F_M$. The $M = 0$ mode can be absorbed into (9.1) by translating t, but now the translational invariance in x must be used in a different way: since

$$H_1 = \frac{\partial H_2}{\partial x} \tag{9.10}$$

we can translate x in the $M = 2$ mode, rather than in f, to eliminate A_1, again leaving $M = 2$ dominant. Similarly for (9.6), we have

$$\lambda_M = \frac{n+1-m}{2(1-n)} + M, \tag{9.11}$$

with

$$F_0 = \eta^{\frac{n+1-m}{m+1-n}}, \qquad F_M = -\lambda_{M+1}F_{M+1} + \frac{m+1-n}{2(1-n)}\eta\frac{dF_{M+1}}{d\eta}. \tag{9.12}$$

Here F_0 can be absorbed into (9.1) (within, as always here, the linearisation) by a translation of x, and the $M = 1$ mode suppressed by translation of t in H_2, given that

$$H_1 = \frac{\partial H_2}{\partial t}.$$

The above somewhat lengthy discussion is motivated both by the crucial role such arguments have implicitly played in the degree-of-freedom counts that have formed an important part of our analysis and by their broader implications for the application of symmetry methods in a variety of contexts.

We conclude with the following remarks. We claim that the collection of potential types of singular behaviour illustrated by Figure 1 is rather comprehensive for PDE problems of the class with which we have been concerned. Our results thus confirm the power of self-similar approaches in addressing such phenomena. Similarity solutions are central to the analysis addressed above, but it is equally important to stress that these need not be similarity solutions to the original PDE – in many cases they involve the taking of an asymptotic limit (associated either with linearisation about an exceptional exact solution or simply with neglect of specific terms) prior to an appeal to self-similarity. The current example is notably rich in the range of possibilities that can be realised in terms of the interface velocities, these covering the full range from zero to unbounded. It is thus likely that it would be extremely challenging to establish rigorous regularity results on these moving-boundary problems.

References

[1] Angenent, S., Aronson, D., Betelu, S. & Lowengrub, J. (2001) Focusing of an elongated hole in porous medium flow. *Phys. D* **151** (2-4), 228–252.

[2] Barenblatt, G. I. (1996). *Scaling, Self-Similarity, and Intermediate Asymptotics: Dimensional Analysis and Intermediate Asymptotics*, Cambridge University Press, Cambridge.

[3] Bluman, G. W. & Cole, J. D. (2012). *Similarity Methods for Differential Equations*, Springer New York, New York, **13**.

[4] Crank, J. & Gupta, R. S. (1972) A moving boundary problem arising from the diffusion of oxygen in absorbing tissue. *IMA J. Appl. Math.* **10** (1), 19–33.

[5] Foster, J. M., Gysbers, P., King, J. R. & Pelinovsky, D. E. (2018) Bifurcations of self-similar solutions for reversing interfaces in the slow diffusion equation with strong absorption. *Nonlinearity* **31** (10), 4621–4648.

[6] Foster, J. M. & Pelinovsky, D. E. (2016) Self-similar solutions for reversing interfaces in the slow diffusion equation with strong absorption. *SIAM J. Appl. Dyn. Syst.* **15** (4), 2017–2050.

[7] Foster, J. M., Please, C. P., Fitt, A. D. & Richardson, G. (2012) The reversing of interfaces in slow diffusion processes with strong absorption. *SIAM J. Appl. Math.* **72** (1), 144–162.

[8] Galaktionov, V. A., Shmarev, S. I. & Vazquez, J. L. (1999) Regularity of interfaces in diffusion processes under the influence of strong absorption. *Arch. Rat. Mech. Anal.* **149** (3), 183–212.

[9] Galaktionov, V. A., Shmarev, S. & Vázquez, J. L. (2000) Behaviour of interfaces in a diffusion-absorption equation with critical exponents. *Interface Free Bound.* **2** (4), 425–448.

[10] V. A. GalaktionovS. R. Svrshchevskii 2006, *Exact Solutions and Invariant Subspaces of Nonlinear Partial Differential Equations in Mechanics and Physics*, Chapman and Hall/CRC.

[11] Galaktionov, V. A. & Vazquez, J. L. (1994) Extinction for a quasilinear heat equation with absorprtion i. technique of intersection comparison. *Commun. PDEs* **19** (7-8), 1075–1106.

[12] Galaktionov, V. A. & Vazquez, J. L. (1994) Extinction for a quasilinear heat equation with absorption II. A dynamical systems approach. *Commun. PDEs* **19** (7-8), 1107–1137.

[13] Grundy, R. (1992) The asymptotics of extinction in nonlinear diffusion reaction equations. *J. Austral. Math. Soc. B* **33** (4), 414–429.

[14] Hulshof, J., King, J. R. & Bowen, M. (2001) Intermediate asymptotics of the porous medium equation with sign changes. *Adv. Diff. Eqns.* **6** (9), 1115.

[15] Ji, H. & Witelski, T. P. (2017) Finite-time thin film rupture driven by modified evaporative loss. *Phys. D* **342**: 1–15.

[16] Kalashnikov, A. S. (1974) The propagation of disturbances in problems of non-linear heat conduction with absorption. *USSR Comp. Math. Math. Phys.* **14** (4), 70–85.

[17] Kersner, R. (1983) Nonlinear heat conduction with absorption: Space localization and extinction in finite time. *SIAM J. Appl. Math.* **43** (6), 1274–1285.

[18] King, J. R. (1992) Local transformations between some nonlinear diffusion equations. *J. Austral. Math. Soc. B* **33** (3), 321–349.

[19] King, J. R. & Please, C. (1986) Diffusion of dopant in crystalline silicon: An asymptotic analysis. *IMA J. Appl. Math.* **37** (3), 185–197.

[20] Lacey, A. (1983) Initial motion of the free boundary for a non-linear diffusion equation. *IMA J. Appl. Math.* **31** (2), 113–119.

[21] Lacey, A., Ockendon, J. & Tayler, A. (1982) "Waiting-time" solutions of a nonlinear diffusion equation. *SIAM J. Appl. Math.* **42** (6), 1252–1264.

[22] Mimura, M., Matano, H. & Chen, X.-Y. (1995) Finite-point extinction and continuity of interfaces in a nonlinear diffusion equation with strong absorption. *J. Reine Angew. Math.* **459**: 1–36.

A Special cases of (1.1)

Special cases of (1.1) are worth recording here, in part for providing some pointers towards the reasons for the demarcating roles of $n = 1$ and $m + n = 1$, though they are not otherwise of significance in the above.

Three cases can be written in divergence form, implying the potential presence of two conserved quantities for each (depending on the boundary conditions, of course). These are as follows.

(I) $n = 0$:

$$\frac{\partial h}{\partial t} = \frac{\partial^2}{\partial x^2}\left(\frac{1}{m+1}h^{m+1} - \frac{1}{2}x^2\right), \tag{A.1}$$

the potential conserved quantities being, as in the case of (II) below, the mass $\int h\,dx$ and the first moment $\int xh\,dx$. For $m = -2$, $n = 0$ the potential-hodograph transformation takes (1.1) to Burgers' equation which can in turn be mapped to the heat equation by the Cole-Hopf transformation.

(II) $n = 1$:

$$\frac{\partial}{\partial t}(e^{-t}h) = \frac{\partial^2}{\partial x^2}\left(\frac{1}{m+1}e^{-t}h^{m+1}\right). \tag{A.2}$$

Here the changes of variable

$$h = e^{-t}\phi, \qquad \tau = \frac{1}{m}(e^{mt} - 1), \tag{A.3}$$

transform (1.1) to the porous-medium equation,

$$\frac{\partial\phi}{\partial t} = \frac{\partial}{\partial x}\left(\phi^m\frac{\partial\phi}{\partial x}\right), \tag{A.4}$$

implying the presence of further symmetry.

(III) $n = m + 1$: In this case,

$$\frac{\partial}{\partial t}(e^{\pm(m+1)^{1/2}x}h) = \frac{\partial}{\partial x}\left(e^{\pm(m+1)^{1/2}x}\left(h^m\frac{\partial h}{\partial x} \mp \frac{1}{(m+1)^{1/2}}h^{m+1}\right)\right), \tag{A.5}$$

and the two conserved quantities are $\int e^{\pm(m+1)^{1/2}x}h\,dx$. In the subcase $m = -4/3$, $n = -1/3$, the changes of variables

$$H = \exp(\mp\sqrt{3}ix)h, \qquad X = \frac{\sqrt{3}}{2}i\exp\left(\pm\frac{2i}{\sqrt{3}}x\right) \tag{A.6}$$

map (1.1) to

$$\frac{\partial H}{\partial t} = \frac{\partial}{\partial X}\left(H^{-4/3}\frac{\partial H}{\partial X}\right). \tag{A.7}$$

implying the presence of two further symmetries; that (A.6) involves complex quantities would seem likely to limit the applicability of these, however. For $m < -1$, linear combinations of (A.5) lead to real expressions involving trigonometric functions.

Introducing the 'pressure' variable $v = h^m$ transforms (1.1) to

$$\frac{\partial v}{\partial t} = v\frac{\partial^2 v}{\partial x^2} + \frac{1}{m}\left(\frac{\partial v}{\partial x}\right)^2 - mv^{\frac{m+n-1}{m}}, \tag{A.8}$$

which comes in three quadratically nonlinear guises, namely when $n = 1$ (see (II) above), $n = m + 1$ (see (III) above) or $m + n = 1$. In consequence, invariant subspaces of solutions are available; see [10] and references therein. For $n = m + 1$ (i.e. case (III) above) these solutions to (A.8) take the form, up to a translation in x,

$$v = \left(a(t) - b(t)\cosh\left(\frac{mx}{(m+1)^{1/2}}\right)\right)_+ \tag{A.9}$$

where the functions $a(t)$ and $b(t)$ satisfy the coupled ODEs

$$\frac{da}{dt} + ma^2 + \frac{m}{m+1}b^2 = 0, \qquad \frac{db}{dt} + \frac{m(m+2)}{m+1}ab = 0$$

and $a > b > 0$ for $m > 0$ and $a > 0$, $b < 0$ for $m < 0$. For the case $m + n = 1$, these solutions to (A.8) take the form

$$v = \left(a(t) - b(t)x^2\right)_+ \tag{A.10}$$

where the functions $a(t)$ and $b(t)$ satisfy the coupled ODEs

$$\frac{da}{dt} + 2ab + m = 0, \qquad \frac{db}{dt} + \frac{2(m+2)}{m}b^2 = 0$$

For $m + n = 1$ and $m > 0$, a special case of solution to (A.8) is an additional double reduction (travelling-wave and scaling) giving rise to the one-parameter family

$$v = \frac{m}{2}\left((c^2 + 4)^{1/2} + c\right)(ct - x)_+ \tag{A.11}$$

with arbitrary constant c that, significantly, can take either sign (with $c > 0$ for $-\partial v/\partial x > m$ and $c < 0$ for $-\partial v/\partial x < m$). Pairs of exponents at the intersection of two or more of the above special cases are $m = 0$, $n = 1$ ((II), (III) and $n + m = 1$, equation (1.1) then being linear; the other linear case, $m = 0$, $n = 0$, does not arise in such a fashion, $m = 1$, $n = 0$ ((I) and $m + n = 1$) and $m = -1$, $n = 0$ ((I) and (III)).